OXIDANT- INDUCED INJURY IN THE MAMMALIAN MYOCARDIUM: FUNCTIONAL AND MOLECULAR EFFECTS OF ACETAMINOPHEN

by

KATHRYN MICHELLE JAQUES

A Dissertation submitted to the

Graduate School-New Brunswick

Rutgers, The State University of New Jersey

and The Graduate School of Biomedical Sciences

University of Medicine and Dentistry of New Jersey

in partial fulfillment of the requirements for the degree of

Doctor of Philosophy

Graduate program in Physiology and Integrative Biology

written under the direction of

Gary F. Merrill, Ph.D.

and approved by

_____

_____

_____

_____

_____

New Brunswick, New Jersey

May, 2010

ABSTRACT OF THE DISSERTATION

Oxidant-Induced Injury in the Mammalian Myocardium:

Functional and Molecular Effects of Acetaminophen

by KATHRYN MICHELLE JAQUES

Dissertation Director:
Gary F. Merrill, Ph.D.

For over 100 years, acetaminophen (APAP) has been exclusively used as an efficacious antipyretic and analgesic. Here we report our ongoing investigation of the cardiovascular effects of APAP. In the first part of this study, we investigated the effects of 15 mg/kg APAP on hydrogen peroxide (H_2O_2)-induced canine myocardial dysfunction *in vivo*. Respiratory, metabolic, and hemodynamic indices such as left ventricular function (LVDP and $\pm dP/dt_{max}$), and percent ectopy were measured in anesthetized, open-chest dogs during intravenous administration of increasing doses of H_2O_2. Following 6.6 mM H_2O_2, tissue from the LV was harvested for electron microscopy. APAP-treated dogs regained greater fraction of baseline function after high concentrations of H_2O_2. Moreover, the incidence of H_2O_2 -induced ventricular arrhythmias was reduced in APAP-treated dogs. Additionally, electron micrograph images of left ventricular tissue confirmed preservation of tissue ultrastructure in APAP-treated hearts.

In the second part of this study, we investigated the effects of APAP on doxorubicin (DOX)-induced murine cardiac fibrosis *in vivo*, with a more detailed investigation of osteopontin (OPN) involvement using the H9c2 myocyte cell line *in*

vitro. We hypothesized that APAP would attenuate DOX-induced reactive oxygen species (ROS) and subsequent fibrosis via attenuation of increased cardiomyocyte OPN synthesis. In H9c2 cells, we found a dose-dependent decrease in cell viability at all concentrations of DOX, which was attenuated by 50 μM APAP. Increased ROS was observed at all concentrations of DOX, which also was attenuated by APAP. A trend of DOX-induced increased OPN RNA synthesis was observed, and was significantly decreased in the presence of APAP. Additionally, in WT and OPN-/- mice receiving four weekly injections of 4 mg/kg DOX ± APAP (30 mg/kg), we found increased fibrosis in groups receiving DOX as compared to those receiving DOX + APAP. Furthermore, fibrosis in WT mice was higher than OPN-/- mice after DOX. Our results support the following conclusions: APAP is protective against (1) H_2O_2 –induced canine myocardial dysfunction, (2) H_2O_2 –induced arrhythmias, and (3) DOX injury by decreasing ROS, and (4) lowering OPN RNA synthesis. (5) The absence OPN and presence of APAP decrease the severity of myocardial fibrosis due to DOX injury.

ACKNOWLEDGEMENTS

I would like to express my gratitude to the members of my committee: Drs. David T. Denhardt, Harvey R. Weiss, Jianjie Ma, Richard J. Leone and Gary F. Merrill for their generous donation of time and guidance in the pursuit of my doctoral degree.

I would also like to specifically thank the following individuals: Dr. Gary F. Merrill for his guidance and support throughout my graduate studies; Dr. David T. Denhardt for his mentorship, guidance and generous donation of both time and resources; Dr. Roseli Golfetti for her friendship and inspiration; Dr. Norell Hadzimichalis, Sunanda Baliga, and Dana Cifelli for their friendship, inspiration, support and collaboration on the study.

Finally, I wish to thank my husband, Raymond E. Robinson, my parents, Susan E. Jaques, Dr. David G. Jaques, and Robin L. Jaques, and my sister and brother, Sarah E. Jaques-Ross and Richard Ross for their guidance, patience, encouragement, support, and love, and my friends and family for their undying support and love. Without these people, I can definitely state that none of this would be possible. Thank you.

TABLE OF CONTENTS

LIST OF TABLES

LIST OF FIGURES

ABBREVIATIONS

$\pm dP/dt_{max}$ …….… Left Ventricular Function

APAP ……...… Acetaminophen

CAF ……...……. Collagen Area Fraction

DOX ……. Doxorubicin

ECM ……..…….. Extracellular Matrix

H_2O_2 …….. Hydrogen Peroxide

HR ……..……. Heart Rate

LV …….…… Left Ventricle

LVDP ……...…. Left Ventricular Developed Pressure

MI …….…… Myocardial Infarction

MMP-2 ……. Matrix Metalloproteinase-2

MMP-9 ……...….. Matrix Metalloproteinase-9

$\cdot O_2^-$ ……. Superoxide

$OH^\cdot$ ……. Hydroxyl Radical

OPN …….. Osteopontin

P_{CO2} …….……. Partial Pressure of Carbon Dioxide

P_{O2} ……. Partial Pressure of Oxygen

ROS ……...…….. Reactive Oxygen Species

SAP ……..…….. Systemic Arterial Pressure

SR ……. Sarcoplasmic Reticulum

INTRODUCTION

1. BACKGROUND

1.1 Brief History of Acetaminophen

For over 100 years, acetaminophen (paracetamol; APAP, N-Acetyl-para-Amino-phenol) has been exclusively used as an efficacious antipyretic and analgesic [1-3]. Cahn and Hepp inadvertently discovered its therapeutic properties while trying to treat intestinal worms using naphthalene [4, 5]. The first clinical use of the drug is ascribed to Hinsberg and Treupel (1894), who showed that a 500 mg oral dose of acetaminophen was effective as an antipyretic, and required lower doses to exert its antipyretic effects than other agents currently available (e.g. phenacetin, antipyrine). However, as a new drug, the choice for analgesics/antipyretics remained aspirin, phenacetin and acetanilide despite these promising findings [5]. Acetaminophen was rediscovered by Brodie and Axelrod in 1949 as a metabolite of acetanilide and phenacetin. Shortly after, it gained popularity among scientists and doctors and was first marketed in the United States around 1950, and subsequently marketed in the United Kingdom in 1956 [5, 6]. Since, more extensive investigation has found acetaminophen to be as effective as aspirin in reducing fever and pain caused by radiant heat, cancer, dental surgery, or arthritis. Further studies confirmed the safety of this drug claiming that, unlike other popular analgesic agents of the time such as aspirin, acetaminophen did not produce gastrointestinal toxicity. Today acetaminophen remains one of the leading over-the-counter drugs used for reducing both fever and pain [7].

More recently, investigators have begun to scrutinize the effects of acetaminophen outside of its traditional properties. For example, Baliga *et al.* [8] investigated the effects of acetaminophen on cerebral ischemia-reperfusion-induced injury using a transient global forebrain ischemia model. Male Sprague-Dawley rats received 15mg/kg of acetaminophen intravenously during ischemia induced by hypovolemic hypotension and bilateral common carotid arterial occlusion, which was followed by reperfusion. Acetaminophen reduced tissue damage, degree of mitochondrial swelling, and loss of mitochondrial membrane potential. Acetaminophen maintained mitochondrial cytochrome *c* content and reduced activation of caspase-9 and the incidence of apoptosis. Rahme and colleagues [9] investigated the effects of acetaminophen in combination with gastroprotective agents in the stomach, a study which was spurred by Nakamoto *et al.* [10] who focused on the effects of acetaminophen on acute gastric mucosal injury mediated by ischemia, and found that the drug was cytoprotective in this environment. In the renal system, Farquhar *et al.* [11] established that renal dysfunction in the stressed human kidney is attenuated in acetaminophen versus ibuprofen-treated patients. Hinson *et al.* [12] and Lores Arnaiz *et al.* [13] found that acetaminophen, although normally associated with hepatotoxicity at excessive doses due to the formation of free radicals, at subthreshold concentrations, acts as an antioxidant in many tissues. They attributed the antioxidant properties of acetaminophen as most likely due to its phenolic structure (Figure 1). Further studies have recently investigated the effects of acetaminophen in the reproductive system [14] and skeletal muscle [15].

A

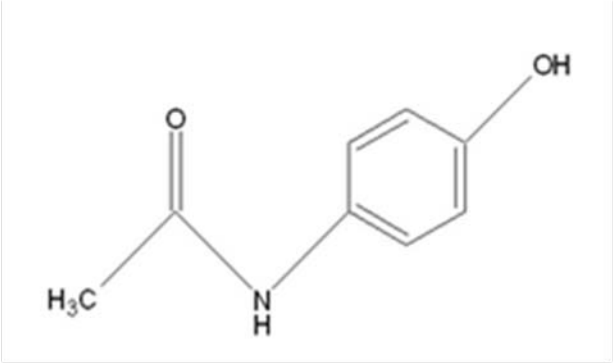

B

Figure 1. Acetaminophen. (A) Chemical structure and (B) space-filling model of acetaminophen (paracetamol, APAP). The benzene ring core is substituted by one hydroxyl group, which distinguishes this compound as a phenol.

1.2 Acetaminophen in the Cardiovascular System

In recent studies acetaminophen has been reported to exhibit cardioprotective efficacy when administered during ischemia/reperfusion, hypoxia/reoxygenation, or exogenous peroxynitrite administration. For example, in our lab, we have found both chronic and acute acetaminophen treatment to be cardioprotective following ischemia/reperfusion in the isolated perfused guinea pig myocardium [16-19]. In vivo, we have also demonstrated that acute acetaminophen treatment provides protection in a canine model of myocardial infarction [20].

Both functional and structural myocardial preservation was observed in chronic and acute administrations of acetaminophen using isolated and perfused guinea pig hearts [16-19, 21]. In chronic studies, guinea pigs were administered acetaminophen-treated drinking water ad libitum for 10 days. Hearts were subsequently extracted and subjected to 20 min of low flow global myocardial ischemia followed by 40 min of reperfusion. Golfetti and colleagues [16] established that hearts chronically treated with acetaminophen demonstrated significantly greater retention of LVDP, attenuation of reactive oxygen species, and preserved myofibrillar ultrastructure when compared to vehicle-treated hearts.

For the acute studies, acetaminophen-treated hearts (0.35 mM) were exposed to 20 min of low flow global myocardial ischemia followed by 40 min of reperfusion, as with the chronic studies. We found that acetaminophen-treated hearts exhibited greater preservation of mechanical function (i.e. left ventricular developed pressure, LVDP), myofibrillar ultrastructure, and significant attenuation of reactive oxygen species when compared to non-treated hearts [19]. Additional work showed that creatine kinase

activity (an indicator of tissue damage) was also significantly reduced during reperfusion in acetaminophen-treated hearts [18]. These studies in our lab over the past decade suggest that the mechanical, structural, and biochemical cardioprotective efficacy of acetaminophen during ischemia/reperfusion extends from an acute to a chronic environment.

Canine studies corroborate these findings and further demonstrate the cardioprotective efficacy of acetaminophen following ischemia/reperfusion. Merrill *et al.* [22] examined hearts in the presence or absence of acetaminophen (total dose, 30 mg/kg iv) in dogs subject to 1 h left anterior descending coronary artery occlusion followed by 3 h of reperfusion. At the completion of the experiment, hearts were simultaneously stained with Evan's blue dye and triphenyltetrazolium chloride to visualize viable tissue outside and inside the area at risk, respectively. Upon examination, acetaminophen-treated hearts were found to have significantly more viable tissue, a greater ability to attenuate peroxynitrite levels in coronary venous effluent, and visibly preserved myofibrillar ultrastructure than hearts not treated with acetaminophen. These results demonstrate the translational utility of *ex vivo* studies to the *in vivo* arena.

Further support from recent reports by Zhu and colleagues [23] corroborate these data. These investigations utilized rats, subject to daily intraperitoneal injections of 5 mg/kg/day acetaminophen 7 days prior to surgery (permanent left coronary artery ligation) and extending until 2 days following the surgery. Mortality rates following myocardial infarction of acetaminophen treated rats were 21.5% versus 37.5% in non treated rats. Triphenyltetrazolium chloride staining was also used in this investigation to show a significant reduction in left ventricular infarct size in acetaminophen-treated

versus non-treated rats (31.3% versus 44.8%, respectively). Additionally, electrocardiograms of treated rats 10 days post-treatment showed noticeable reductions in ST segment elevation (an indicator of electrical damage following myocardial infarction).

Acetaminophen was also evaluated in the setting of hypoxia/reoxygenation by Rork *et al.* [20]. In these studies we exposed isolated perfused guinea pig hearts to 6 min of hypoxia followed by 36 min of reoxygenation and examined hemodynamic, metabolic, mechanical, ultrastructural, and biochemical indices of function. Results indicated that acetaminophen-treated hearts retained significantly greater mechanical function, preserved myofibrillar ultrastructure, and a significantly greater ability to neutralize peroxynitrite-dependent chemiluminescence at all recorded time periods. In addition, creatine kinase activity was significantly decreased during both hypoxia and reoxygenation in acetaminophen-treated hearts. We concluded that the cardioprotective efficacy of acetaminophen (0.35 mM) could be extended from an ischemia/reperfusion environment to also include myocardial protection from hypoxia/reoxygenation injury.

Numerous studies involving acetaminophen in ischemia/reperfusion, drug, and oxidant-induced arrhythmogenesis have confirmed similar cardioprotection. Recent work from Merrill *et al*. [21] examined the effects of therapeutic acetaminophen treatment on either oubain- or ischemia/reperfusion -induced ventricular arrhythmias in dogs. We found that acetaminophen-treated dogs experienced a significant decrease in overall percent ectopy. These studies were spurred by previous work from Merrill and Goldberg [19] which suggested that acetaminophen can attenuate sodium pentobarbital induced ventricular arrhythmias *ex vivo*. Acetaminophen-treated guinea pig hearts analyzed for ventricular salvos and ventricular premature beats for 90 min post sodium

pentobarbital administration were found to be significantly less arrhythmic when compared to non-treated hearts.

For a number of years, mechanistic evidence of acetaminophen-mediated cardioprotection has been notably lacking. Recently, Hadzimichalis *et al*. [21] investigated the effects of acetaminophen on Langendorff-perfused guinea pig hearts exposed to acute treatment with acetaminophen (0.35 mM) or vehicle (saline) beginning at 15 min of a 30-min baseline stabilization period. Low-flow global myocardial ischemia was subsequently induced for 30 min followed by 60 min of reperfusion. Mitochondrial swelling and mitochondrial cytochrome *c* release were assessed and found to be significantly and completely reduced in acetaminophen- vs. vehicle-treated hearts following reperfusion. In a separate group of hearts, ventricular myocytes were isolated and subjected to fluorescence-activated cell sorting. Acetaminophen-treated hearts showed a significant decrease in late stage apoptotic myocytes compared with vehicle-treated hearts following injury (58 +/- 1 vs. 81 +/- 5%, respectively). Additionally, Rork *et a.l* [24] have shown that acetaminophen attenuates peroxynitrite-activated matrix metalloproteinase-2-mediated troponin I cleavage via direct inhibition of peroxynitrite in ischemia/reperfused guinea pig hearts. While this work is promising, additional mechanistic data are essential to further characterize the role of acetaminophen in providing myocardial protection in cases of other pathology resulting in oxidative injury.

1.3 Reactive Oxygen Species

Chemistry

Reactive oxygen species (ROS) are, generally speaking, oxygen molecules in different states of oxidation or reduction. ROS include free radicals and biologically active compounds, such as hydrogen peroxide (H_2O_2), that can be converted to radicals. The term "free radical" refers to an atom or molecule that can exist independently, if briefly, with one or more unpaired electrons. By virtue of their unpaired electron, free radicals are typically unstable, highly reactive, and short-lived. Free radicals are generated by one electron reduction or oxidation of molecules creating an unpaired electron. In normal mitochondrial oxidative phosphorylation, O_2 is reduced by four electrons to form H_2O. The energy derived from this reduction of O_2 serves to meet the energy demands of the cell. Paradoxically, it is also the actual process of oxygen reduction that leads to the formation of oxygen free radicals (reactive oxygen species, ROS). Incomplete reduction of O_2 leads to the generation of superoxide anion ($\cdot O_2^-$), hydrogen peroxide (H_2O_2), and hydroxyl radical ($OH\cdot$). $\cdot O_2^-$ is unstable with a lifetime of milliseconds at neutral pH, and in aqueous solution it spontaneously reacts or dismutates to yield H_2O_2 and O_2. The $OH\cdot$ is an extremely reactive and short -lived free radical produced in biological systems. In the Haber-Weiss reaction, O_2 and two $OH\cdot$ are formed when $\cdot O_2^-$ reacts spontaneously with H_2O_2. In the Fenton reaction (iron-catalyzed Haber-Weiss reaction), reduction or oxidation of a trace metal in the presence of $\cdot O_2^-$ and H_2O_2 gives rise to $OH\cdot$. Hydrogen peroxide, as opposed to $\cdot O_2^-$ and other ROS, is a highly stable small molecule that freely crosses membranes as its biological diffusion properties are similar to water [25].

Biological Significance

ROS have an important role in several important biological processes under subtoxic conditions. They are involved in a variety of cellular signaling pathways ("redox signaling") [26], acting in some instances as second messengers downstream of certain ligands including TGF-β1, PDGF, ATII, FGF-2, endothelin and others [27-29]. They are believed to interact with cell signaling pathways by way of modification of key thiol groups on proteins that possess regulatory functions such as serine/threonine kinases, tyrosine kinases and mitogen-activated protein kinases (MAPKs), growth factors and transcriptions factors. For example, ROS modulates the activity of NF-κB, GATA4, and the activator protein-1 (AP-1). NF-κB, for example, becomes more transcriptionally active in response to the contribution of ROS to the degradation of IκB, the inhibitory partner of NF-κB that sequesters it in the cytosol. Conversely, GATA4 (which regulates cardiac sarcomere proteins) activity is reduced in response to ROS. H_2O_2, specifically, regulates the catalytic activity of enzymes by redox modification of cysteine residues [30]. These include tyrosine phosphatase activity, the translocation and activation of serine/threonine kinases such as PKC and the induction of gene expression.

Under physiologic conditions, ROS are produced in moderation during cellular respiration allowing endogenous antioxidant defenses (i.e: catalase, SOD, and glutathione) to neutralize these compounds before causing irreversible damage. However, at toxic levels, these endogenous antioxidant defenses are overwhelmed and allow ROS to contribute to tissue injury. For example, mutagenesis of DNA may occur by inducing strand breaks, purine oxidation, and protein-DNA cross-linking. These and other ROS-mediated alterations in chromatin structure may significantly affect gene

expression. Also, ROS are responsible for oxidant-induced calcium overload [31, 32] mediated by a variety of mechanisms. *In vitro*, H_2O_2 has been demonstrated to activate Na^+-Ca^{2+} exchange, either fatigue [33] or enhance L-type Ca^{2+} currents [31], increase Na^+-H^+ exchange [34, 35], and induce Ca^{2+} -induced Ca^{2+} release from the SR (sarcoplasmic reticulum) [36] in cardiac myocytes. Additionally, modification of proteins by ROS can cause inactivation of critical enzymes and can induce denaturation that renders proteins nonfunctional.

Ischemia/Reperfusion-induced Oxidant Injury

A number of mechanisms have been shown to mediate post-ischemia, reperfusion-induced, myocardial injury. The most prevalent mechanism involves oxidative stress [37] wherein an overabundance of reactive oxygen species (ROS) damage cardiomyocyte lipid membranes, nucleic acids, proteins and carbohydrates and interfere with intra- and intercellular signaling pathways [38, 39]. Reperfusion overwhelms the mitochondria with oxygen, causing them to undergo higher rates of metabolism in an effort to restore ischemia-mediated ATP depletion. The vast number of oxidants produced as a result of the high metabolic rate of the mitochondria overpowers endogenous antioxidant defenses. Compelling evidence for a role for ROS injury comes from an array of sources. The oxygen paradox hypothesis was first introduced in 1973 when it was demonstrated that reoxygenation of the hypoxic rat heart resulted in significant damage rather than improvement [40]. Second, Lucas *et al.* [41], Stewart *et al.* [42], and Jolly *et al.* [43] substantiated this concept in the canine and the rabbit model of global ischemia/reperfusion using known oxygen radical scavengers. In these studies,

the ability of oxygen radical scavengers to improve mechanical, sarcoplasmic reticulum, and mitochondrial function suggested that oxygen free radicals participate in experimental ischemia/reperfusion injury. Third, by perfusing an oxygen radical generating system in an isolated rabbit heart preparation, Burton *et al.* [44] directly demonstrated oxygen radical induced myocardial damage. Subsequently, Ytrehus *et al.* [45] also demonstrated deleterious effects of oxygen radicals in isolated rat hearts. Fourth, by developing sensitive and specific electron paramagnetic resonance methods, [46] direct measurement and characterization of the free radical generation following reperfusion of the ischemic myocardium was possible. Fifth, a more recent clinical study demonstrated that oxygen radical scavenging is effective in preventing reperfusion-induced arrhythmias [47]. Likewise, transgenic overexpression of superoxide dismutase (SOD) has been shown to reduce infarct size in mice following myocardial infarction (MI) [48]. However, attempts to target SOD to improve outcome after MI in other animal models have yielded mixed results, suggesting that ROS activation is only a single contributor to post-MI necrosis and reperfusion injury and/or that SOD alone is insufficient to neutralize the deleterious effects of ROS in this setting.

Exogenous H_2O_2 is commonly used as a source of oxygen-derived free radicals, specifically $OH^{\cdot}$, to study the effects of the reperfused ischemic myocardium [31, 49]. Josephson and colleagues [31] tested the hypothesis that oxidants and oxygen radicals can cause cardiac myocyte injury and intracellular calcium overload, using isolated adult rat ventricular myocytes and exposed them to H_2O_2 (1-10 mM) and Fe3(+)-nitrilotriacetate. Electron paramagnetic resonance measurements confirmed the production of the highly reactive $OH^{\cdot}$ radical by this system. The oxygen radical

generating system initially caused a transient augmentation of twitch amplitude in single field stimulated myocytes. This was followed by contractile oscillations occurring during the twitch prior to full cell relaxation, and spontaneous mechanical oscillations occurring between electrically stimulated contractions. Eventually, cells became inexcitable and abruptly underwent contracture. In the presence of lower bathing calcium concentrations, these oxidant-induced alterations were prevented or delayed. However, cells exposed to the radical generating system in the absence of extracellular calcium still eventually underwent contracture but stimulated contractions or mechanical oscillations were not seen. Measurements in single myocytes loaded with the fluorescent probe of intracellular calcium, Indo-1, demonstrated a rise in both systolic and diastolic fluorescence ratio, as well as oscillations and widening of the fluorescence transient, suggestive of cellular calcium loading, following exposure to the radical generating system.

Doxorubicin-induced Oxidant Injury

Doxorubicin (DOX), an anthracycline antibiotic, has been widely used in the treatment of a variety of tumors and carcinomas. Its anti-neoplastic activity is conferred by two key features: sequence-selective DNA intercalation and inhibition of topoisomerase II. The planar structure allows for intercalation between paired bases in the DNA helix. This non-covalent interactin is strong enough to inhibit DNA and RNA synthesis, and perhaps plays a central role in activating apoptotic pathways via DNA damage. DNA damage at levels below that necessary to trigger cell death may lead to cumulative cardiotoxicity via accumulation of DNA mutations, particularly in mitochondria. Anthracyclines also cause DNA damage through their activity as

topoisomerase poisons. In the late 1970's and early 1980's, it was discovered that anthracyclines would induce strand breaks in DNA of L1210 leukemic cells through association with proteins later identified to be topoisomerase II. Topoisomerase is a key enzyme involved in DNA synthesis that alters the topology of DNA without altering sequence. The supercoiling of the DNA double helix is changed depending on the cell cycle phase and the transcriptional activity. DOX acts by stabilizing a reaction intermediate in which DNA strands are cut and covalently linked to tyrosine residues of topo II, inhibiting DNA resealing. DNA damage is followed by growth arrest in GI and G2 and programmed cell death.

However, clinical application of DOX is limited by its irreversible cardiac side effect of cardiomyopathy and congestive heart failure. The ultra-structural changes seen in endomyocardial biopsies of patients with DOX-associated heart failure include loss of myofibrils, disarray of sarcomere structure, dilation of the sarcoplasmic reticulum, swelling of the mitochondria and cytoplasmic vacuolization. Although not completely understood, an attractive mechanism is the hypothesis that DOX-induced cardiotoxicity involves the loss of cardiac myocytes via one of several pathways of death. In this model, there is DOX-induced myocyte loss with each dose. Given the limited regenerative capacity of the heart, cumulative toxicity at some point surpasses a threshold of irreparable damage that triggers a more generic process of ventricular remodeling common to multiple forms of cardiac injury [50].

Anthracycline treatment of cultured cardiac myocytes has been shown to induce cell death in a concentration-dependent manner [51, 52]. Recent studies have demonstrated release of cytochrome *c* with anthracycline treatment in a rat myocyte cell

line (H9c2) and *in vivo* [53, 54]. The mechanism of cell death varies with concentration, with apoptosis occurring at lower and necrosis at higher doxorubicin concentrations. Work in animals and humans has demonstrated that generally apoptotic cell death occurs after *in vivo* exposure to doxorubicin and involves a mitochondrial pathway involving Bax, cytochrome *c*, and caspase-3 [55-57].

The underlying mechanism of cell death is thought to be attributed to oxidative damage. Anthracyclines are known to result in generation of cellular oxidative stress, and this has been proposed as a proximal step leading to myocyte cell death. Specifically, the quinone functionality of DOX is transformed in the presence of NADH into the semiquinone via one-electron reduction by complex I of the electron transport chain [58]. The semiquinone form reacts with molecular oxygen to produce a superoxide radical, whereby DOX returns to the quinone form. The cycling of DOX between quinone and semiquinone forms generates large amounts of superoxide, which further give rise to a variety of active ROS species, including H_2O_2 $OH\cdot$, and $ONOO^-$ (Figure 2) [59]. Oxidative stress alone is sufficient to induce myocyte death as well as activation of the 'fetal gene program' that is a feature of many forms of heart failure (i.e. induction of atrial natriuretic peptide [ANP] and brain natriuretic peptide [BNP]). Many studies have led to the idea that oxidative stress may play a central role in the pathogenesis of chronic cardiac remodeling after any form of injury. In the setting of anthracycline exposure, increased generation of ROS is known to occur. For example, hydroxyl radical formation in the intact heart increases in the presence of DOX and can be inhibited by treatment with superoxide dismutase, catalase and the iron chelator, dextrazoxane [60]. Clinically,

the only drug known to prevent doxorubicin-induced heart injury is dextrazoxane which has also been shown to inhibit DOX-induced troponin elevation [61].

Cellular stress, and specifically oxidative stress, activates a host of kinase pathways that appear important in determining cell fate, and these pathways likely modulate the response of the heart to anthracycline exposure. Mitogen/stress activated protein kinases (MAPKs and SAPKs) have been proposed as a cellular mediator linking anthracyclines to the apoptotic pathway and the myocardial remodeling pathway. MAPKs deliver extracellular signals from activated receptors to effector proteins, such as transcription factors, to direct gene expression, or other regulators of cell function that play a fundamental role in survival, proliferation, and apoptosis. In cardiac myocytes, ERK is activated by growth factors/hypertrophic agents and thought to mediate cell survival. The SAPKs JNK and p38 are activated by cellular stresses and correlate with cardiac myocytes apoptosis. Recent data also suggests that ROS production can activate these pathways, in particular JNK and p38, supporting the association of anthracyclines and SAPK mediated apoptosis.

Another potential mechanism by which the DNA-damaging effects of DOX could lead to secondary cardiotoxicity is via the suppressed transcription of sarcomeric proteins. GATA4 is a member of the zinc finger transcription factor family, important in regulating differentiation, sarcomere synthesis, as well as survival signaling. GATA4 is expressed in the heart and regulates several cardiac specific genes as well as a number of anti-apoptotic genes [62-64]. GATA4 is also a survival factor for differentiated postnatal cardiac myocytes [65] and an upstream activator of the antiapoptotic gene Bcl-X_L. Many GATA4 regulated genes, including cardiac adriamycin-responsive protein (CARP), atrial

natriuretic protein (ANP), troponin I, and alpha-myosin heavy chain, are suppressed by anthracycline treatment, suggesting an interaction between DOX and GATA4 activity [66, 67]. Similar to other zinc finger transcription factors, GATA4 DNA binding activity is inhibited by ROS production. Treatment with DOX down-regulates GATA4 expression in isolated rat cardiac myocytes and the HL-1 cardiac cell line, and ectopic expression of GATA4 attenuates the incidence of apoptosis [68]. GATA4 contains a conserved MAPK phosphorylation site at serine 105 within the transcriptional activation domain. Serine 105 of GATA4 is phosphorylated in response to agonist stimulation through ERK1/2, and weakly through JNK or p38 MAPKs.

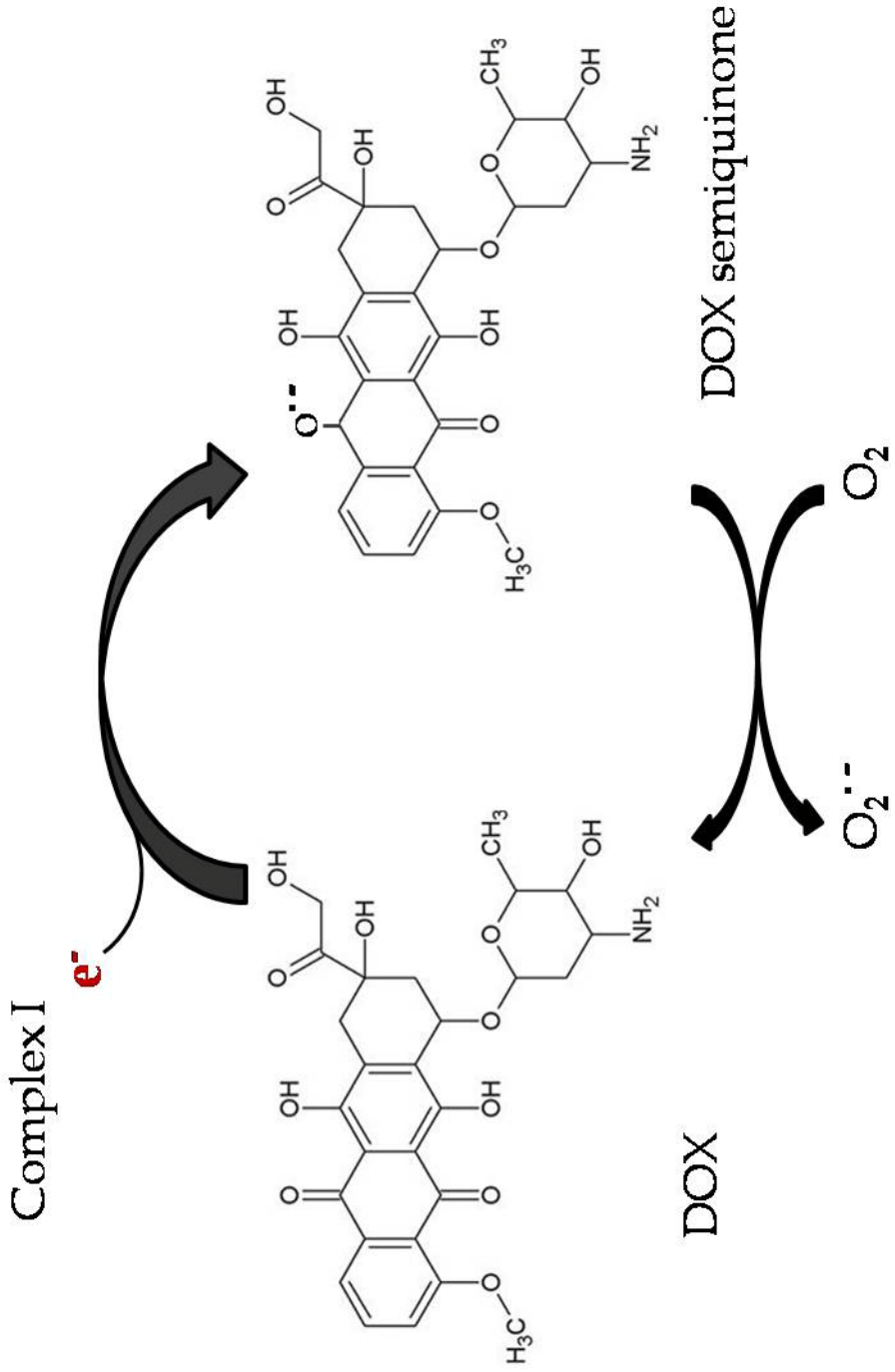

Figure 2: Formation of doxorubicin semiquinone by single electron transfer from ETC Complex I.

1.4 Consequences of Oxidant-Injury in the Cardiovascular System

Cardiomyocyte Apoptosis

Cardiomyocyte apoptosis occurs in hypertrophied, ischemic and failing hearts and may contribute to the development and progression of cardiac dysfunction. Experimental evidence suggests that ROS can mediate apoptosis by a variety of mechanisms, including direct mediation of genotoxicity. Interestingly, ROS-mediated induction of apoptosis appears to be concentration dependent. For instance, in adult cardiomyocytes, relatively low levels of H_2O_2 are associated with the activation of ERK1/2 MAPK and the stimulation of protein synthesis. Conversely, higher levels of H_2O_2, while still activating ERK1/2, also activates the JNK and p38 MAPKs and Akt and induces apoptosis [69]. Takimoto et *al.* further described ROS-mediated activation of ERK1/2 and subsequent induction of apoptosis signaling kinase-1 (ASK1) triggering NF-κB and AP-1 which results in matrix metalloproteinase (MMP) expression. Studies using ASK1-deficient mice confirmed decreased cellular apoptosis and ventricular remodeling after MI [70].

Cardiac Excitation-Contraction

In addition to the longer-term effects of altering cellular transcription, ROS are also capable of triggering rapid changes in protein function as a result of altering the redox state of the proteins. In cardiac myocytes, rapid changes in cellular oxygen can contribute to electrophysiological instability in the myocardium and the development of arrhythmias. ROS can also directly influence contractile function by modifying proteins central to excitation-contraction coupling. This includes modification of critical thiol groups (-SH) on the ryanodine receptor to enhance its open probability, suppression of L-

type calcium channel current, and oxidative and nitrosative interaction with the sarcoplasmic reticular Ca^{2+} ATPase to inhibit Ca^{2+} uptake. Oxidants have been shown to stimulate Ca^{2+} signaling by increasing cytosolic Ca^{2+} concentration, suggesting a possible physiological role of oxidants in the regulation of Ca^{2+} -signaling. Enhanced Ca^{2+}-transport through Ca^{2+} channels as well as the inhibition of Ca^{2+} -pumps occur in the presence of oxidants, and these macromolecules may be possible target sites of oxidants to elicit Ca^{2+} signaling [31].

Reports show direct interactions between the Ca^{2+} channels and oxidants, which result in Ca^{2+} release from the SR of cardiac and skeletal muscles. H_2O_2 (3-5 mM) increased the open probability of sheep cadiac SR Ca^{2+} -release channel without affecting the conductance of the channel under voltage-clamp conditions [71]. More recently it was observed that physiological (μM) concentrations of H_2O_2 stimulate Ca^{2+}-induced Ca^{2+} release from SR of freshly isolated whole cell-clamped rat ventricular myocytes dialyzed with fura-2, and this appears to be due to the action of H_2O_2 on the SR Ca^{2+} channel [72]. Additionally, H_2O_2 (100μM) increased plasmalemmal Ca^{2+} leak channel activity which may be attributed to the increased intracellular Ca^{2+} [73].

The importance of Na^+ current in electrical and contractile dysfunction was demonstrated using rabbit and guinea pig isolated ventricular myocytes exposed to 200 μM H_2O_2. An increase in I_{Na} due to H_2O_2 contributed to Ca^{2+} and Na^+ overload and decreased contractile relaxation, which was reversed by selectively blocking the late I_{Na} with Ranolazine [74].

Ventricular Remodeling: Cardiac Fibrosis

Under nonpathological conditions the balance of collagen synthesis and degradation is crucial to the homeostasis of the extracellular matrix. Cardiac adaptation in response to intrinsic or external stress involves a complex process of chamber remodeling including structural changes in the myocardial wall, and myocyte molecular modifications. Physiologically, ventricular remodeling is a compensatory response that enables the heart to adapt to increased stress, but may quickly turn maladaptive and pathologic.

At least 20% of patients who suffer MI go on to develop heart failure, and approximately 26% of patients develop heart failure after cumulative DOX treatment [75]. The manner in which the ventricle heals and remodels after injury is a major determinant of eventual cardiac function and the progression to heart failure. ROS may contribute to the remodeling process in a number of ways, including inducing synthesis of osteopontin (OPN) and MMPs that participate in reconfiguration of the extracellular matrix; acting as signaling molecules in the development of compensatory hypertrophy; and contributing to myocyte loss via apoptosis or other cell death mechanisms [76, 77]. Recently it was shown that inhibition of xanthine oxidase with allopurinol after experimental MI in dogs diminished ROS production in the myocardium and attenuated maladaptive LV remodeling, leading to improved post-MI cardiac function [78].

Streeter and Basset [79, 80], using a structural engineering approach, demonstrated that myocyte orientation and myocardial fiber angles are highly organized and move in a continuous fashion from the endocardium to the epicardium. The structural network of matrix proteins is composed of proteins of highly organized structure and

architecture, such as type I and type III collagen, which provide structural integrity to adjoining myocytes and contribute to overall LV pump function through the coordination of myocyte shortening. Further research demonstrated that the myocardial extracellular matrix (ECM) maintains alignment of myofibrils within the myocyte through a collagen-integrin cytoskeleton-myofibril relation [81, 82]. In addition to a fibrillar collagen network, and a basement membrane composed of proteoglycans and glycosaminoglycans, the myocardial ECM contains a large reservoir of bioactive molecules [83, 84]. Certain signaling molecules that have a significant effect on the ECM have been termed matricellular factors and include OPN and thrombospondin (TSP). These factors can function as both a cell attachment molecule as well as a cytokine.

OPN is a secreted phosphoprotein found in body fluids (e.g. plasma, urine, milk) and matrix of mineralized tissues. Its expression is minimal in normal adult cardiomyocytes and fibroblasts and functions as a matricellular protein to maintain extracellular matrix (ECM) integrity, but increases during pathological events such as tissue remodeling during injury [85]. After being translated, OPN is phosphorylated by a member of the golgi casein-kinases, sugar chains added to it, and is then secreted out of the cell. The function of secreted OPN can be altered by proteases including thrombin, allowing it to function as an immobilized matrix molecule or a soluble cytokine. OPN binding to transmembrane integrins and CD44 initiates signaling pathways ultimately responsible for cell-matrix and cell-cell interactions such as cell adhesion, chemotaxis, and signaling [86]. OPN promotes cell attachment and migration through its recognition as a ligand by several cell adhesion receptors, e.g., integrins avb3 and avb5 [87, 88].

Additionally, binding of OPN to the β_1-integrin receptors, promotes the adrenergically-mediated atrial natriuretic peptide (ANP) response in cardiomyocytes [89].

The functional importance of OPN in the heart is not known. Some researchers maintain it plays an integral role in tissue protection and regeneration [90], while others argue it contributes to exacerbated scar formation and pathologic conditions. Following ischemia/reperfusion injury, OPN synthesis is increased in the heart [91, 92]. In mice and humans, increased OPN expression has been linked to post-MI left ventricular remodeling by promoting collagen synthesis and accumulation [92, 93]. Consequently, myocardial hypertrophy (secondary to MI) is highly correlated with increased OPN levels [94]. Conversely, arguments are made in favor of OPN's crucial role in organization of cardiomyocytes and recruitment of newly synthesized matrix after damage, without which, the impacted area would not successfully regenerate [95]. Using OPN -/- mice, Trueblood and colleagues [92] found increased left ventricular chamber dilation, decreased myocyte length, and decreased type I collagen content following MI compared to WT. OPN has also been found as a requirement for angiogenesis following cardiac injury [96].

MMPs are a group of proteins found in the matrix of tissues and are synthesized in response to cellular stress such as oxidative injury. MMPs exert effects central to fibrosis and remodeling in the heart. MMP-2 and MMP-9, are endoproteinases implicated in cardiac remodeling and when overexpressed or not counterbalanced by tissue inhibitors of matrix metalloproteinases, initiation into heart failure via destruction of collagen and ultimately cell to matrix contacts. MMP-2 and MMP-9 are gelatinases that demonstrate substrate affinity for denatured fibrillar collagen, basement membrane

proteins such as collagen type IV, fibronectin, and laminin. MMP-2 and MMP-9 also exhibit proteolytic activity against elastin and proteoglycans. Most MMPs are secreted from the cell in an inactive pro-peptide form and are activated post-translationally by ROS from targeted interactions with critical cysteines in the propeptide autoinhibitory domain. [97].

2. PURPOSE

2.1 ACETAMINOPHEN IN THE H_2O_2-INJURED MYOCARDIUM

The purpose of the first part of this study was to investigate the effects of acetaminophen on the H_2O_2-injured mammalian myocardium. It is well established that H_2O_2, in addition to other ROS, contribute to myocardial dysfunction in ischemia and reperfusion [98]. In recent investigations our laboratory has shown that acetaminophen has cardioprotective properties in the mammalian myocardium under conditions of ischemia and reperfusion. It has been suggested that these cardioprotective properties are mediated by the antioxidant nature of the drug (phenolic structure), and its ability to attenuate damaging oxygen radicals and nitrating compounds such as superoxide and $ONOO^-$ [99].

While acetaminophen's role in myocardial ischemia and reperfusion injury is becoming clearer, little or no attention has been paid to the specific effects of individual oxidants generated by MI injury *in vivo*. For example, Karmazyn and colleagues [100] reported beneficial effects of NSAIDs on the mechanical function of the *in situ* hypoxic mammalian myocardium, but did not test the efficacy of acetaminophen, which is not an NSAID. In addition, Teng *et al.* [101] have shown that phenols such as urate protect the (homogenized) heart during hypoxia by reducing the influence of damaging oxidants such as $ONOO^-$.

We therefore aimed to identify the cardiac injury caused specifically by H_2O_2, and examined the metabolic, hemodynamic, structural and mechanical effects of acetaminophen on the H_2O_2-injured mammalian myocardium to investigate any putative cardioprotective effects of the drug *in vivo.*

2.2 ACETAMINOPHEN IN THE DOXORUBICIN-INJURED MYOCARDIUM

The second part of this study was to investigate the effects of acetaminophen on the DOX-injured mammalian myocardium and examine the mechanisms of cardioprotection mediated by acetaminophen. It has been well documented in animal and human studies that treatment with DOX induces cardiac dysfunction, cell death and fibrosis [67, 102, 103]. The most widely accepted mechanism of cardiac injury is through production of ROS which induce mitochondrial damage, DNA breaks, sarcomere structural alterations, and altered gene expression in myocytes.

Osteopontin (OPN) is a phosphoglycoprotein whose expression is minimal in normal adult cardiomyocytes and fibroblasts but increases during pathological events such as tissue remodeling during ROS-mediated injury. OPN expression has been linked to post-MI left ventricular remodeling by promoting collagen synthesis and accumulation. This adaptive response to injury is at first beneficial, but can quickly turn pathological when excessive interstitial collagen accumulates. This disequilibrium of the muscular and collagenous compartments of the heart, termed fibrosis, can lead to abnormal myocardial stiffness and eventual heart failure [104].

The effects of APAP on OPN regulation and collagen accumulation are unknown. Perhaps through the attenuation of ROS, acetaminophen is able to concomitantly attenuate the induction OPN and subsequent fibrotic response. Therefore, if acetaminophen is able to decrease levels of ROS, the mechanism of its apparent cardioprotection against fibrosis may be through inhibition of OPN synthesis and subsequent upregulation of interstitial collagen accumulation.

We therefore examined the effects of DOX in WT and OPN-/- mice and on H9c2 cardiac myoblasts in the presence and absence of APAP. We induced fibrosis in mice over 5 weeks using intraperitoneal injections of DOX. We then treated H9c2 cells to DOX ± APAP and investigated cell viability, intracellular oxidant stress, and transcription of OPN.

MATERIALS AND METHODS

1.1 ACETAMINOPHEN IN THE H_2O_2- INJURED MYOCARDIUM

Animals

All experiments were performed on male mongrel dogs weighing 22±0.5kg. Dogs were obtained from licensed vendors, and housed in AAALAC-accredited facilities where room temperature, humidity, and lighting were controlled. Daily rations of Purina Dog Chow and water were provided *ad libitum*. Dogs were allowed several days to acclimate to their new housing conditions and were fasted for 24h prior to the day of experimentation (water provided *ad libitum*). Institutional review and approval of protocols were obtained before initiating experiments and conforms to the *Guide for the Care and Use of Laboratory Animals*.

Surgical preparation and instrumentation

Hair was clipped from the inguinal region, the chest, and on the fore- and hindlimbs in the vivarium, then dogs were transported to the experimental laboratory where they were anesthetized with propofol (6.5 mg/kg i.v.). Immediately following induction of general anesthesia, they were intubated and placed on isoflurane anesthesia (Aerrane, Isoflurane, USP, Baxter; Deerfield, IL) administered in supplemental oxygen at an MAC of 2.0±0.5 per cent and flow rate of 2.0±0.5 liters per minute (Matrix Calibrated Vaporizer, model VIP 3000; Orchard Park, NY; in-line with a Veterinary Anesthesia Ventilator, 2000 ml adult bellows, model 2002IE, Hallowell EMC; Pittsfield, MA).

The right femoral artery and vein were isolated and cannulated [polyethylene (PE)-240 catheters filled with 0.9% NaCl solution] so that monitoring of systemic arterial blood pressure (Pā, pulsatile and mean) and fluid administration (500 U/kg heparin, H_2O_2, acetaminophen and saline) could occur in each vessel respectively. A left-sided thoracotomy was performed and lobes of the left lung were retracted and the pericardium incised. A short, 18g angiocatheter (BD Angiocath Autoguard; Sandy, Ut) was then placed in the left ventricular chamber via the apical dimple. This was used to monitor left ventricular developed pressure (LVDP) and its derivative ($\pm dP/dt_{max}$). A standard 3-lead limb electrocardiogram was attached and used to determine heart rate. Dogs were then allowed time (~20min) for monitored variables to achieve a steady state.

Treatment groups and time course

Two groups of dogs were studied. Both groups were allowed ~20 min to recover from surgical invasion and achieve baseline status. One group was then pretreated with acetaminophen (15 mg/kg, n=10) or an equivalent volume of saline (0.9% NaCl, n=10) (Figure 3). Each pretreatment was administered as an intravenous bolus (15-19 ml), and allowed to circulate for ~15 min. Following the circulation period, both groups were administered incremental concentrations (0.88 mM, 2.2 mM, 6.6 mM) of H_2O_2 (0.88 M H_2O_2 solution, i.v., Target Corporation; Minneapolis, MN) at five-min intervals via the femoral vein. All other variables were monitored continuously.

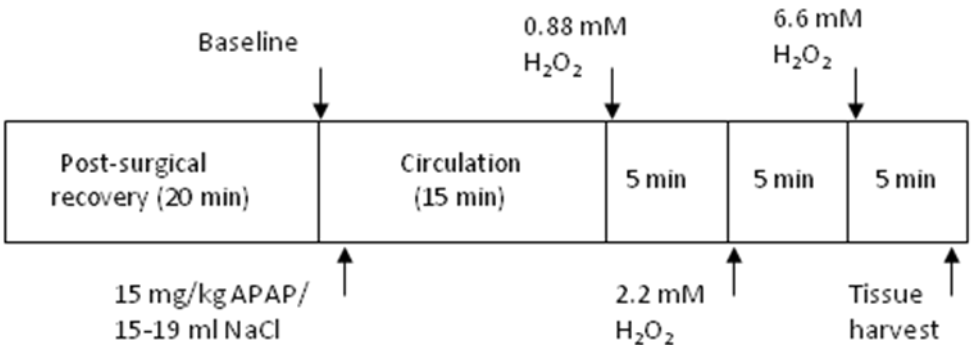

Figure 3: Protocol schematic. All dogs were allowed ~20 min to recover from surgery and achieve stable baseline status. Depending on the group, dogs were administered either 15mg/kg APAP or an equivalent volume of saline and allowed ~15 min to achieve a steady state. Both groups of dogs were administered a low (0.88 mM) concentration bolus of H_2O_2, followed 5 min later by a medium (2.2 mM) concentration bolus, followed 5 min later by a high (6.6 mM) concentration bolus of H_2O_2.

Determination of plasma concentration of acetaminophen

In a third group of dogs (n=6), one bolus injection of 15mg/kg acetaminophen was given via the left femoral vein and allowed to circulate for three hours. Arterial blood samples (i.e: 2-3 ml each) were withdrawn at 0, 30, 60, 90, 120,150, and 180 min after administration of acetaminophen. The blood samples were centrifuged at ~2,000*g* for 10 min, and plasma stored at -70° C. The concentration of acetaminophen in the plasma was determined using validated fluorescence polarization immunoassay performed by a diagnostic laboratory (Quest Diagnostics; Madison, NJ).

Myofibrillar ultrastructure

We examined the myofibrillar ultrastructure of the epi-, and midmyocardium using electron microscopy in H_2O_2 only (n=2) and H_2O_2 + APAP-treated (n=2) dogs. Hearts were arrested using 3M KCl five minutes after administration of 6.6 mM H_2O_2. Immediately following the bolus, a transmural section of myocardium was extracted from the left ventricular free wall adjacent and distal to the third or fourth branch of the left anterior descending artery. Heart sections were then submerged in fixative, and blocks (2-3mm^3) of epi- and midmyocardium were cut. Tissue blocks were fixed with Trumps fixative for 2 hours then postfixed with 1% osmium tetroxide, followed by dehydration in graded ethanol. Samples were embedded in Epon-Araldite cocktail, sectioned with a diamond knife ultramicrotome (model LKB-2088, LKB; Sweden), and viewed with an electron microscope (model JEM-100CXII, JOEL Ltd; Japan) using standard methods. Electronmicroscopic images were digitally acquired and examined for signs of tissue damage.

Monitored variables and data acquisition

For each protocol group, monitored indices included: core temperature (C_t, °C), ventilatory frequency (Vf, cycles/min), tidal volume (Vt, ml), end-tidal CO_2 (percent of expired gases; model NPB-75, Nellcor Puritan Bennett capnograph; Pleasanton, CA), oxyhemoglobin saturation (SaO_2, %, capnography, model NPB-75), blood gasses (PO_2, PCO_2, mmHg; model 248 blood gases/pH analyzer, Chiron Diagnostics; West Haven, CT), electrolytes (K^+, Ca^{2+}, Na^+, EasyLyte Calcium, Medica; Bedford, MA), systemic mean arterial pressure (Pā, mmHg), LVDP (mmHg), and its $\pm dP/dt_{max}$ (mmHg/s), heart rate (HR, cycles/min), and the ECG. All cardiovascular variables were monitored on a CB Sciences data acquisition system (model 214, iWorx; Dover, NH) in series with a computer running Labscribe software (version 6.0, CB Sciences; Dover, NH).

Statistical analysis

All data are presented as mean ± standard error of the mean (SEM). The experiments were designed *a priori*, and Student's t-test for nonpaired replicates was used to identify statistically significant differences between treatment means. Between-group variability was compared using one-way ANOVA followed by Tukey's test for means comparison. Significance was accepted at $P<0.05$.

1.2 ACETAMINOPHEN IN THE DOXORUBICIN-INJURED MYOCARDIUM

Cell Culture

H9c2 rat heart-derived embryonic myocytes were obtained from American Type Culture Collection (ATCC CRL-1446) and cultured in Dulbecco's modified essential medium (Gibco; Carlsbad, CA) supplemented with 10% fetal bovine serum, 2 mM glutamine, 100 units/ml penicillin, 100 μg/ml streptomycin, and 1 mM sodium pyruvate in humidified air (CO_2 5%) at 37°. Cells were kept at or below 70% confluence during culture and allowed to reach 80-90% before experimentation.

Animals

$OPN^{-/-}$ mice in the 129 background were generated and maintained along with isogenic WT controls in the Rutgers Nelson Animal Facility, which is accredited by the Association for Assessment and Accreditation of Laboratory Animal Care and is under the care of a board-certified veterinarian. The research with these mice was approved by the Rutgers Institutional Animal Care and Use Committee veterinarian.

Treatment Groups and Time Course

H9c2 Myoblasts:

Cells were treated with either PBS or acetaminophen (50 μM) for 15 min, incubated with doxorubicin (2 μM, 4 μM, 6 μM, or 8 μM) for 6 h, washed and then switched to fresh medium. At this point, some cells were subject to an oxidative stress

assay (DCFH-DA). Cells used for the cell death assay (MTT), or for PCR analysis were allowed to incubate for an additional 18 h in fresh media (Figure 4).

Animals:

Male 10-12 week-old 129 mice (WT or OPN-/-) were randomly assigned into four groups: (1) saline (n=3), (2) acetaminophen (30 mg/kg; n=3), (3) doxorubicin (4 mg/kg; n=4), or (4) doxorubicin plus acetaminophen (n=4) by intraperitoneal injections weekly for 4 weeks, for a cumulative dose of 16 mg/kg doxorubicin. Following the fifth week, all mice were euthanized by CO_2. Cardiac specimens were then subjected to histological, immunohistochemical, and molecular biological analyses (Figure 5).

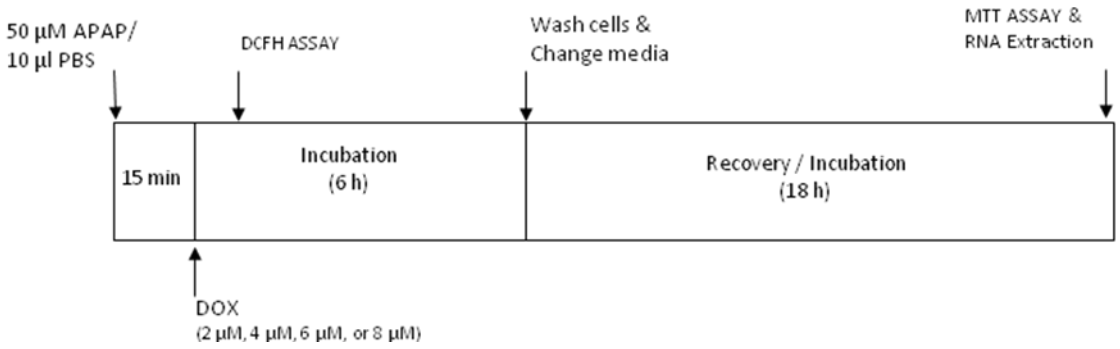

Figure 4: H9c2 protocol schematic. Depending on the group, cells were given either 50 µM APAP or an equivalent volume of PBS and allowed ~15 min to incubate. Cell were then treated with 0 µM, 2 µM, 4 µM, 6 µM, or 8 µM DOX. During the 6 h incubation with DOX, some cells were subject to an intracellular oxidative stress assay (DCFH) where measurements were taken every hour during those 6 hours. For other cell experiments, after 6 h incubation, cells were washed with PBS and fresh medium was replaced. After an additional 18 h, cells were either subject to a cell viability assay (MTT assay), or the RNA was harvested for RT-PCR analysis.

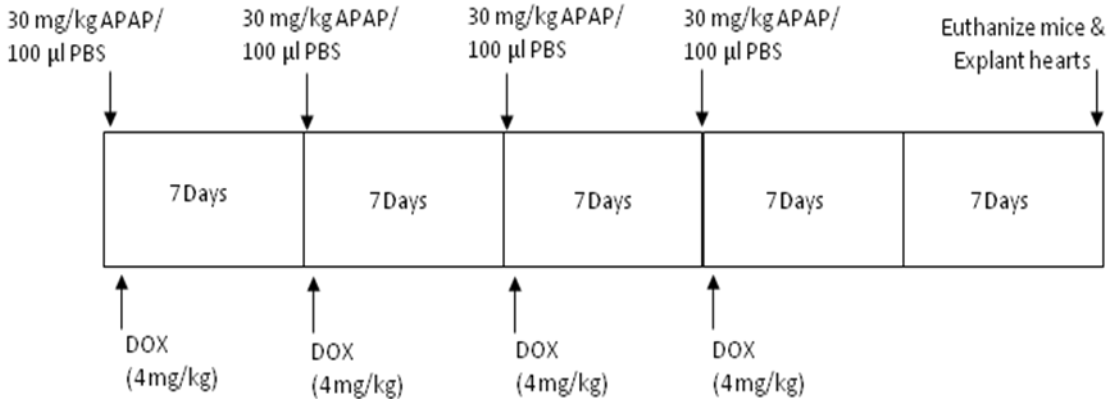

Figure 5: Mouse protocol schematic. Depending on the group, mice were given (IP) either 30 mg/kg APAP or an equivalent volume (~100 µl) of PBS and allowed ~15 min to absorb. Representative mice were then injected with 4 mg/kg DOX. This protocol was repeated every week for 4 weeks. The fifth week, mice were not treated, but allowed an extra week without treatment before explanting hearts.

Cell Viability Assay (MTT)

The viability of cultured cells was evaluated by performing a 3-(4,5-dimethylthiazol-2-yl)-2,5-dephenyltetrazolium bromide (MTT; Sigma; St. Louis, MO) assay as described previously [105]. Briefly, after cells were treated with Dox ± APAP, MTT solution (5 mg/ml in HBSS) was added to a final concentration of 0.25 mg/ml and allowed to incubate for 4 h in the dark at 37º C. Cells with active mitochondria transform MTT into purple formazan crystals. The purple crystals were solubilized in 50 µl DMSO for 1 h. Absorbance of the samples was read using a microplate reader at 570 nm.

Measurement of Intracellular ROS Production: 2',7'-dichlorodihydrofluorescin

The determination of intracellular hydroperoxide production is based on the oxidation of 2',7'-dichlorodihydrofluorescein (DCFH; Sigma-Aldrich; St. Louis, MO) to a fluorescent 2',7'-dichlorofluorescein (DCF) [106]. For quantification of cellular fluorescence, cells were incubated in DMEM (excluding phenol red) on a 12-well plate containing 5 µM DCFH for 30 min. Cells were washed with Hanks Buffered Salt Solution (HBSS; Gibco; Carlsbad, CA) and medium was replaced. Baseline measurements were taken for all wells using a microplate reader at an excitation of 485 nm and emission of 530 nm [107]. Cells were then treated with DOX ± APAP, and measurements were taken every hour for 6 hours. For visual images, cells were treated as above, but images were acquired after 2 h of treatment with DOX ± APAP using a fluorescence microscope with FITC filter.

Total RNA extraction

Total RNA from H9c2 cells was isolated using Trizol Reagent (Invitrogen; Carlsbad, CA). Briefly, 1 ml Trizol was added per 10-cm^2 plate and allowed to sit for 5 min at room temperature. Chloroform was added (0.2 ml/ 1ml Trizol), allowed to sit for 10 min, then centrifuged at 12,000 x *g* for 10 min at 4° C. The aqueous phase was transferred to a fresh tube and mixed with 0.5 ml isopropanol, allowed to sit for 10 min and centrifuged at 12,000 x *g* for 10 min at 4° C. Supernatant was removed and RNA pellet was washed once with 1 ml 75% ethanol by vortexing then centrifuged at 7,500 x *g* for 5 min at 4° C. The RNA pellet was then dissolved in DEPC water for 15 min at 55-60 °C. The final preparation of RNA was tested for purity by spectophotometry and accepted at 260/280 > 1.8.

RT-PCR (Reverse Transcription- Polymerase Chain Reaction)

A 20-µl reaction volume consisting of 2.5 mM 2'-deoxynucleoside 5'-triphosphate mix (dNTP; Invitrogen; Carlsbad, CA), 5 µM N6 random hexamer (Integrated DNA Technologies; Coralville, IA), 5 µg RNA of interest, and sterile H_2O, was added to a 200 µl PCR microcentrifuge tube (Phenix Research Products; Hayward, CA) and heated at 65° C for 5 min in a thermal cycler. Then, 4 µl of 5x first strand buffer and 2 µl of 1 M DTT (Invitrogen; Carlsbad, CA) was added to the reaction and incubated at 25° C for 10 min. Next, 1 µl (200U) Superscript II (Invitrogen; Carlsbad, CA) was added and incubated at 37° C for 50 min. The reaction was inactivated by heating to 70° C for 15 min. The negative control lacked Superscript II.

Four µl of complementary DNA (cDNA) were amplified in a reaction mixture containing 5 µl of 10x PCR buffer (200 mM Tric-HCL pH 8.4, 500 mM KCl), 1.5 µl of 50 mM MgCl, 4 µl of 2.5 mM dNTP mix, 2 µl (10 units) of Taq DNA polymerase, 4 µl of amplification primer mix to gene of interest, and 30.5 µl H_2O in a final volume of 50 µl. The PCR products were analyzed by electrophoresis on a 1.5% agarose gel in Tris-Acetate-EDTA buffer (TAE; 0.04 M Tris-Acetate, 0.001 M EDTA). Densitometric analysis of ethidium-bromide-stained (0.5 µg/ml) agarose gel was carried out by Image J software (NIH; Bethesda, MD). The ratio between the yield of each amplified product and that of the co-amplified internal control allowed a relative estimate of mRNA levels in the sample analyzed. The internal control was GAPDH, a housekeeping gene whose PCR product did not overlap with the studied genes. The two negative controls included a complete reaction setup lacking either cDNA template or Taq DNA polymerase. For OPN amplification we found optimal transcript at 56.5° for 42 cycles using primers: forward, 5'-ACGAGTTTCACAGCCATGAGGACA-3'; reverse, 5'- GCAGTGGCCA TTTGCATTTCTTGC-3' designed using IDT primerQuest software (Coralville, IA).

Histological Analysis

After the fifth week of doxorubicin treatment, mice were euthanized and each heart was removed and fixed in 10% buffered formalin overnight. Hearts were embedded in paraffin, after which 7-µm thick transverse sections were cut using a microtome and plated on poly-L-lysine slides (Sigma; St. Louis, MO). The sections were then rehydrated in an ethanol series and stained with Picro-Sirius Red. Nuclei were stained for 1 min with Weigert's hematoxylin, washed, and then stained for 1 h in 0.1% Sirius

Red stain (Direct Red 80, Sigma; St. Louis, MO) in saturated picric acid. Slides were washed twice in acidified water (5% acetic acid), dehydrated in an ethanol series, and cleared with xylene. Sections were cover-slipped with Permount (Sigma; St. Louis, MO). Images were collected using bright-field microscopy at 10-20 × magnification. Digital images (9-12) of the left ventricular free wall of sections from the apical third, middle, and basal third of each heart were assessed for fibrotic area using Image J software (NIH; Bethesda, MD). Briefly, collagen area fraction (CAF) was measured by dividing the collagen area by the total tissue area of each image.

Statistical analysis

All data are presented as mean ± standard error of the mean (SEM). The experiments were designed *a priori*, and Student's t-test for paired (H9c2 cells) and nonpaired (mice) replicates was used to identify statistically significant differences between treatment means. Between-group variability was compared using one-way ANOVA followed by Tukey's test for means comparison. Significance was accepted at $P<0.05$.

RESULTS

1. ACETAMINOPHEN IN THE H_2O_2-INJURED MYOCARDIUM

1.1 Hemodynamic and Mechanical Properties

Hemodynamic, respiratory, and metabolic indices such as heart rate (HR), partial pressure of oxygen (P_{O2}), and partial pressure of carbon dioxide (P_{CO2}) did not vary significantly between H_2O_2- and H_2O_2 + APAP-treated dogs under baseline or experimental conditions. Circulating Na^+, K^+, and Ca^{2+} levels were also constant throughout the experiment (Table 1). Reported hemodynamic and functional data were analyzed during the first 30 sec after administration of H_2O_2, the time-point which resulted in the most significant cardiovascular responses (Figure 6). Arterial blood samples were collected 5 min after administration of H_2O_2 to allow time for complete mixing and circulation.

At all concentrations of H_2O_2, APAP-treated dogs showed significant preservation of left ventricular function as assessed by left ventricular developed pressure (LVDP) and its derivative ($\pm dP/dt_{max}$) (Figures 7-8). LVDP and its derivative ($\pm dP/dt_{max}$) at baseline did not vary significantly between H_2O_2- and H_2O_2 + APAP-treated dogs. A significant decrease in LVDP was seen in H_2O_2-treated dogs after 6.6 mM H_2O_2 as compared with baseline. This LVDP decrease from baseline was not present in APAP-treated dogs after treatment with 6.6 mM H_2O_2. Specifically, after treatment with 6.6 mM H_2O_2, pressures were 68±3 for H_2O_2 and 79±4 mmHg ($P<0.05$) for H_2O_2 + APAP-treated dogs (Figure 7).

Systolic ($+dP/dt_{max}$) and diastolic ($-dP/dt_{max}$) function were also preserved in H_2O_2 + APAP-treated hearts. Whereas $+dP/dt_{max}$ of H_2O_2-treated animals dropped from

1545±169 to 1355±141 mmHg/s following administration of 6.6 mM H_2O_2, H_2O_2 + APAP-treated animals showed a significant increase, from 1711±90 to 1846±144 mmHg/s (Figure 8) [108].

Table 1: Metabolic and hemodynamic status of anesthetized dogs treated with hydrogen peroxide (H_2O_2) in the presence or absence of acetaminophen

	Baseline		**Baseline + APAP**		**0.88 mM H_2O_2**		**2.2 mM H_2O_2**		**6.6 mM H_2O_2**	
	H_2O_2	**A**	H_2O_2	**A**	H_2O_2	**A**	H_2O_2	**A**	H_2O_2	**A**
Tc ***(°C)***	39	39	38	38	38	38	37± 1	38	37± 1	38
HR ***(cycles/min)***	106± 35	109± 36	106± 35	111± 37	107± 36	110± 37	105± 35	109± 36	103± 34	106± 35
P_{O2} ***(mmHg)***	381± 26	386± 31	381± 26	386± 31	388± 25	376± 28	373± 28	366± 29	320± 33	316± 31
P_{CO2} ***(mmHg)***	41± 1	45± 1.6	41± 1	45± 1.6	43± 1.3	46± 2.1	43± 1.4	47± 2.3	43± 1.3	48± 2.5
Na^+ ***(mEq/L)***	135± 9	141± 1	135± 9	141± 1	143	142± 1	143	142± 1	142	141± 1
K^+ ***(mEq/L)***	4.2± 0.1	4.1± 0.1	4.2± 0.1	4.1± 0.1	4.2± 0.1	4± 0.1	4.1± 0.1	4.1	4.1± 0.1	4± 0.1
Ca^{2+} ***(mEq/L)***	1.4	1.4	1.4	1.4	1.4	1.4	1.4	1.4	1.4	1.4

Note: Data are mean ± SEM (n=10). H_2O_2, hydrogen peroxide; A, acetaminophen; Pā, systemic mean arterial blood pressure; HR, heart rate; PO_2, partial pressure of oxygen; PCO_2, partial pressure of carbon dioxide; Na^+, sodium; K^+, potassium; Ca^{2+}, calcium.

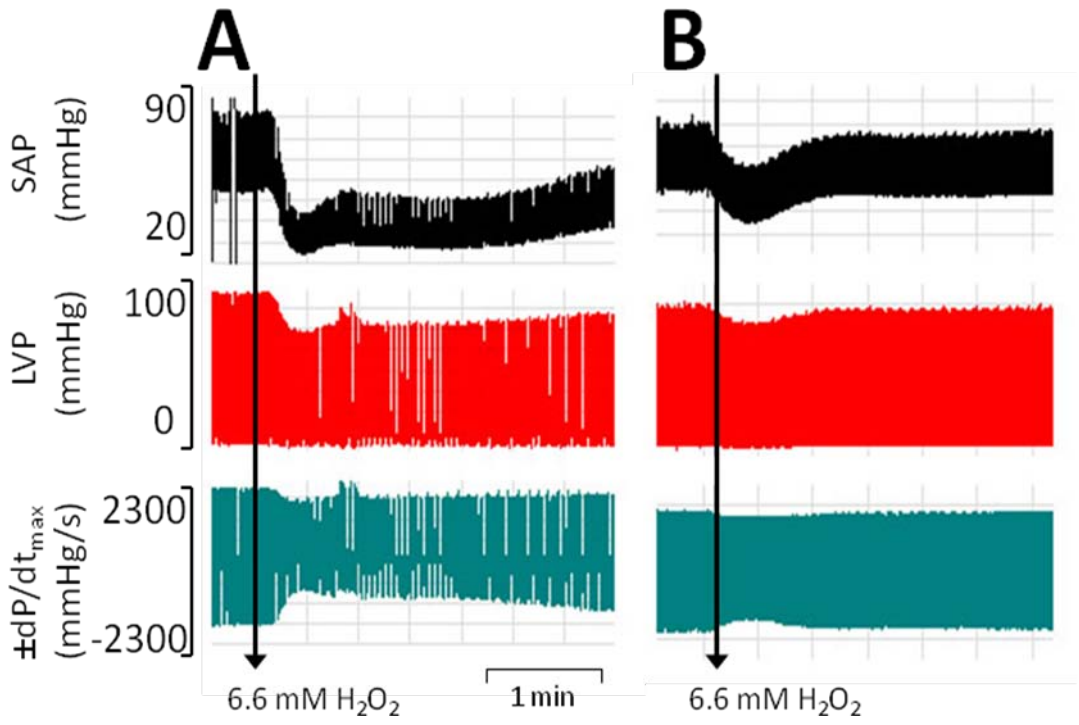

Figure 6: Representative trace of systemic arterial pressure (SAP), left ventricular pressure (LVP) and its derivative ($\pm dP/dt_{max}$) in (A) H_2O_2-and (B) APAP + H_2O_2-treated dogs following administration of 6.6 mM H_2O_2 [108].

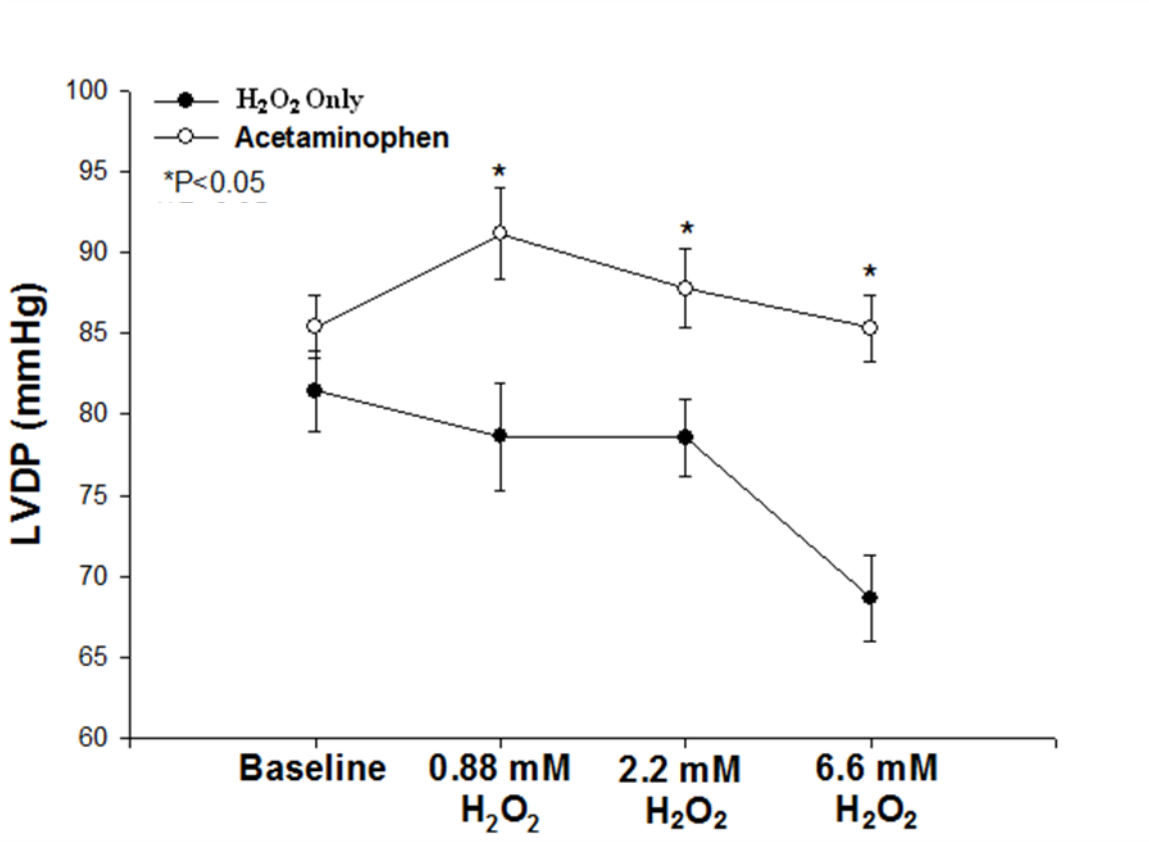

Figure 8: LVDP was retained in APAP- (15mg/kg) versus H_2O_2-only treated dogs (n=10 per group) during administration of increasing concentrations of H_2O_2. *P<0.05 relative to corresponding value for H_2O_2 treatment [108].

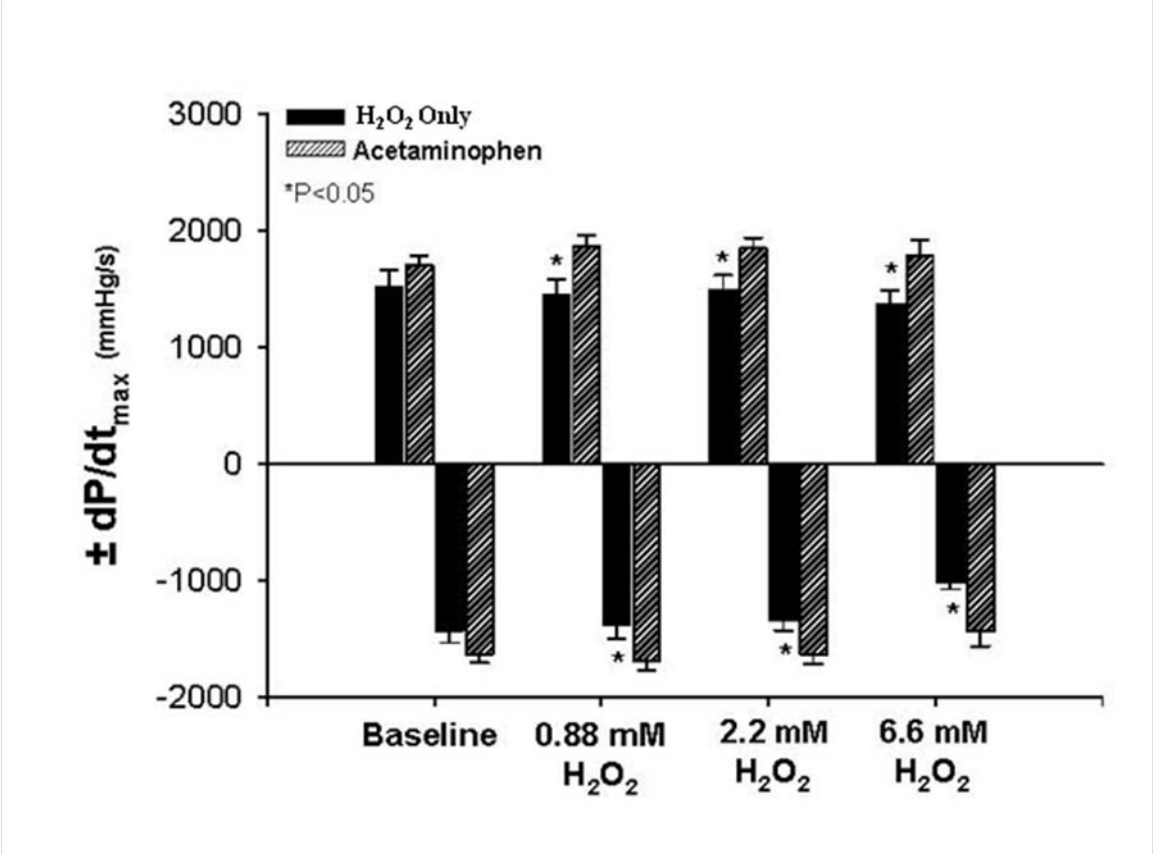

Figure 8: Influence of APAP (15mg/kg) on $\pm dP/dt_{max}$ in H_2O_2-treated dogs (n=10 per group). APAP-treated groups gained or retained systolic function and retained diastolic function compared to H_2O_2-only treated groups. *P<0.05 relative to corresponding value for H_2O_2 treatment [108].

1.2 Electrocardiogram

The severity of arrhythmias was expressed as the percent ectopy: the number of ectopic beats (per min) divided by the total beats (per min) X 100 [109]. The ectopic beats were evaluated from the shape of the QRS complex and its associated relationship to systemic and ventricular pressures based on previously defined guidelines [110].

Heart rate and incidence of ventricular arrhythmias did not vary between groups under baseline conditions. A H_2O_2 concentration-dependent increase in arrhythmias was seen in both groups of dogs, but was significantly attenuated in the presence of APAP. For example, after intravenous administration of 0.88 mM H_2O_2, percent ectopy was 0.39±0.13 in H_2O_2-treated and 0.05±0.02 in H_2O_2 + APAP-treated dogs. Following treatment with 6.6 mM, percent ectopy was 1.04±0.3 in H_2O_2-treated and 0.27±0.1 ($P<0.05$) in H_2O_2 + APAP-treated dogs (Figure 9). This is a 77% decrease in total number of ectopic beats in APAP-treated dogs when compared to H_2O_2-only treated dogs.

Additionally, the occurrence of basal arrhythmia (reflecting the recovery from the surgical intervention) did not vary significantly between H_2O_2- and H_2O_2 + APAP-treated groups. However, immediately following administration of 15mg/kg APAP, percent ectopy decreased significantly in the APAP-treated dogs in the absence of H_2O_2 (Figure 6) [108].

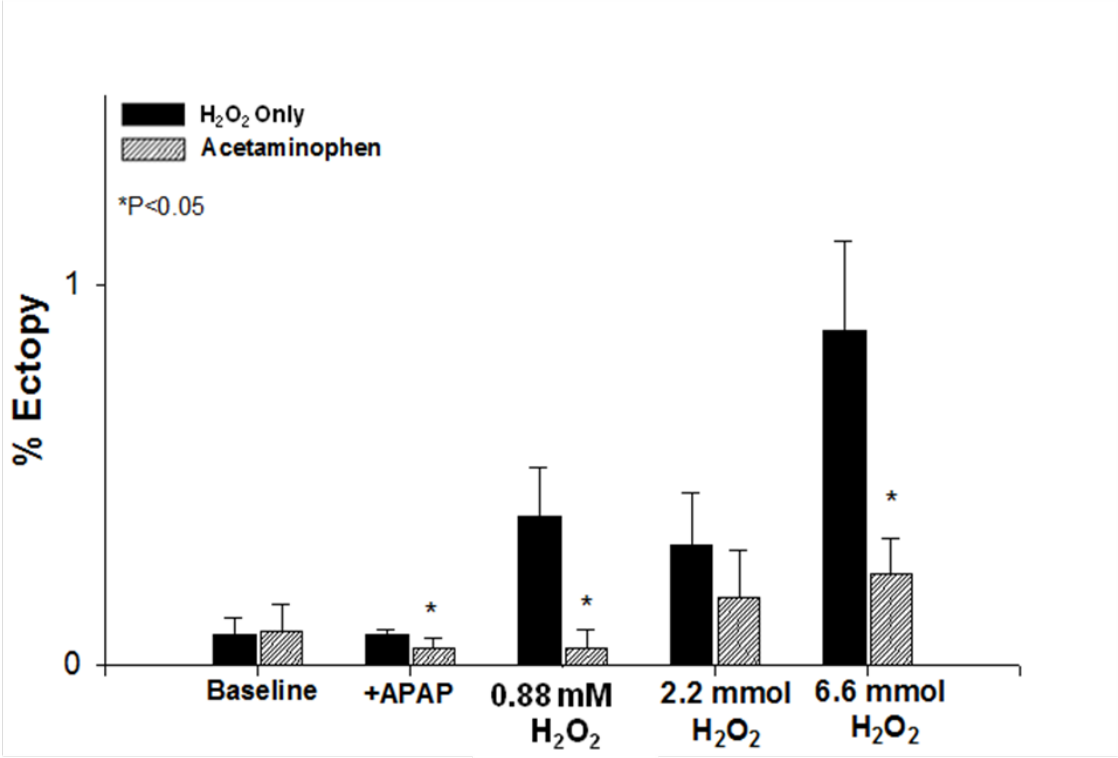

Figure 9: Influence of APAP (15mg/kg) on H_2O_2 -induced arrhythmias (n=10 per group). After 0.88 mM and 6.6 mM of hydrogen peroxide, APAP-treated groups significantly retained a more regular rhythm than H_2O_2-only-treated groups. *P<0.05 relative to corresponding value for vehicle treatment [108].

1.3 Plasma concentration of acetaminophen

The time course for changes in the circulating concentrations of APAP after i.v. administration is shown in Figure 10. The elimination half-life ($t_{1/2}$) of a 15mg/kg APAP bolus was an estimated 55 min. The maximum plasma concentration (Cmax) and the time corresponding to Cmax (Tmax) were 19.1±2 ug/ml and 30 min respectively [108].

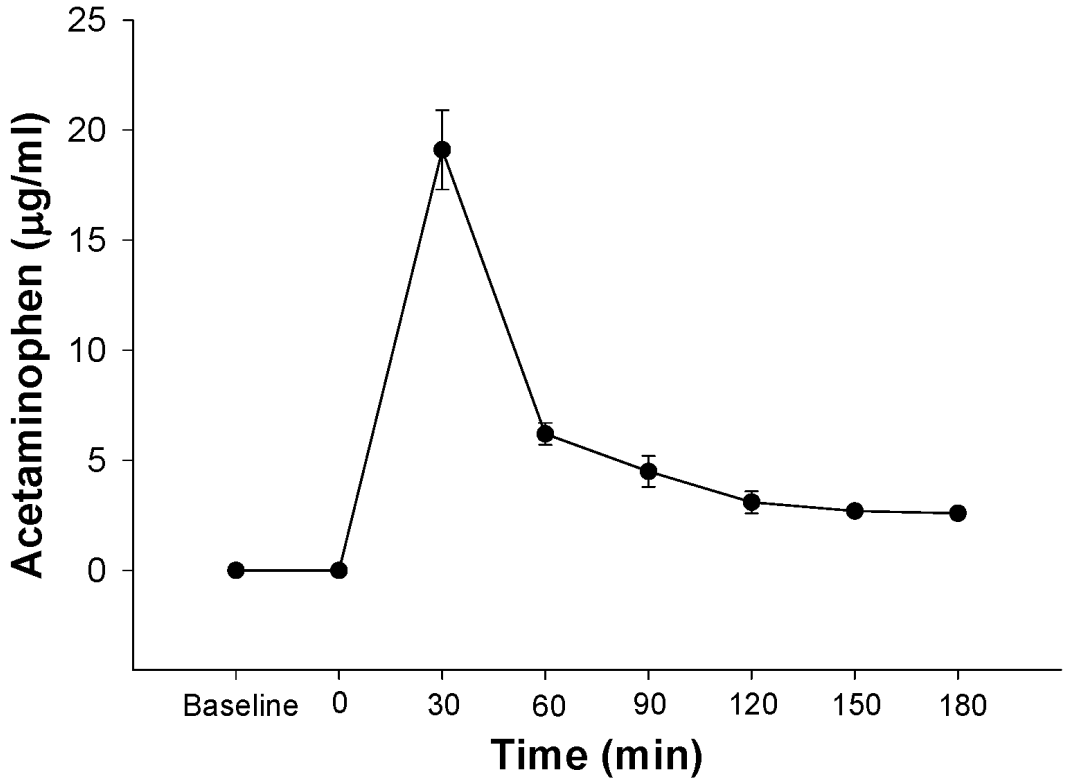

Figure 10: Plasma concentrations of circulating APAP after i.v. administration (15mg/kg). Acetaminophen concentration peaked ~30 min after administration with a corresponding value of 19.1±2 µg/ml, and was nearly fully metabolized after 3 hours [108].

1.4 Myofibrillar Ultrastructure

Following 6.6 mM treatment of H_2O_2, epimyocardial tissue obtained from H_2O_2-only treated hearts showed dilated sarcotubules, mild contracture, liposome deposition, and numerous mitochondrial amorphous matrix densities (AMDs) (Figure 11B). The light I-bands and dark Z-lines within the sarcomere were disjointed and blurred in H_2O_2-treated hearts but well-defined in H_2O_2 + APAP-treated hearts. APAP-treated hearts had less lipid deposition, an absence of vacuoles, more compact cristae and more ordered myofilaments (Figure 11A). Also, the mitochondria did not appear as swollen, were darker, lacked AMDs, and were more densely packed. Examination of midmyocardial tissue exhibited similar signs of damage and protection in H_2O_2- (Figure 11D) and H_2O_2 + APAP-treated (Figure 11C) dogs respectively [108].

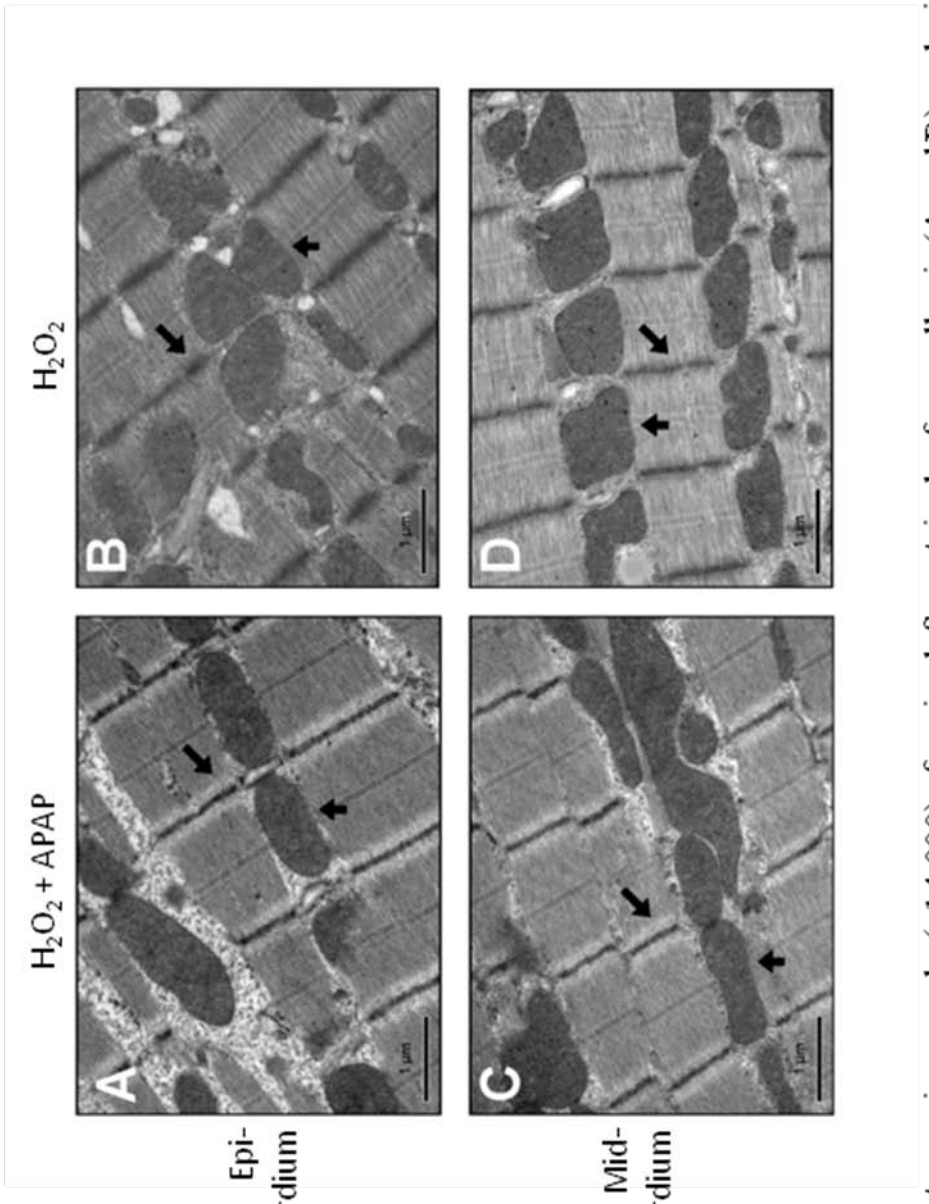

Figure 11: Electron micrographs (x14,000) of canine left ventricular free wall epi- (A and B) and mid-myocardium (C and D) after treatment with 6.6 mM H_2O_2 in the presence (A and C) or absence of APAP (B and D) treated dogs. Note the mitochondria and light/dark bands of sarcomeres.

2. ACETAMINOPHEN IN THE DOXORUBICIN-INJURED MYOCARDIUM

2.1 Cell Viability of Doxorubicin Treated Cardiomyocytes

Doxorubicin-induced toxicity was assessed using the MTT assay on H9c2 cells. Untreated control cells and cells treated with 50 µM APAP did not differ significantly from each other. A dose-dependent decrease in cell viability was observed at all concentrations of DOX. For example, at 4 µM DOX, cells were 87% viable compared to control, at 6 µM were 84% viable and 8 µM were 83% viable. In the presence of DOX + APAP, cells receiving 6 µM (91% viability vs. 85% viability) and 8 µM (88% viability vs. 83% viability) DOX showed significantly increased viability as compared to DOX treatment alone (Figure 12).

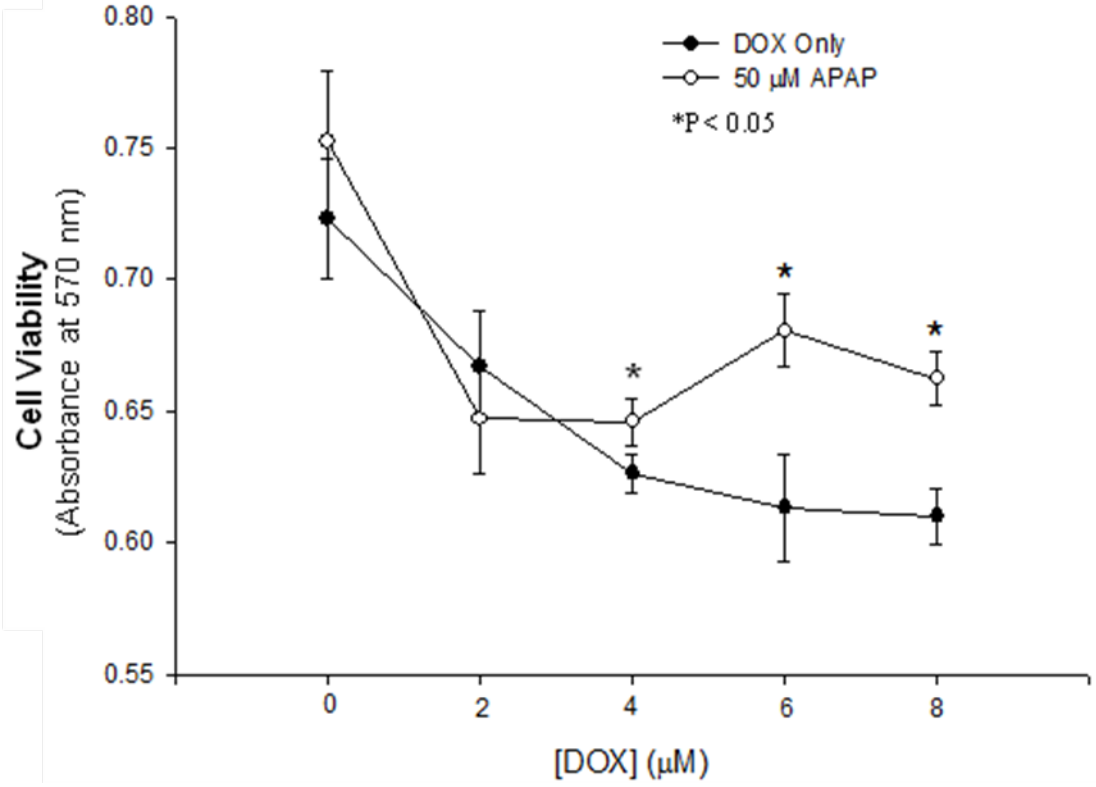

Figure 12: Effect of APAP on cell viability after treatment with increasing concentrations of DOX, as determined by the MTT assay. H9c2 cells grown to 80% confluence were subject to DOX ± APAP for 6 h, medium was changed, and cells were allowed to incubate for an additional 18 h in fresh medium. DOX significantly decreased cell viability at concentrations of 4 µM and above. APAP significantly increased cell viability at DOX concentrations at 4 µM and above. Results represent means of six independent experiments ± SEM. *P < 0.05

2.2 Oxidative Stress in Doxorubicin-Treated Cardiomyocytes

The oxidant action of DOX was confirmed in H9c2 cells by detecting intracellular oxidation of dichlorofluorescein diacetate (DCF). Cells were exposed to 2 µM, 4 µM, 6 µM and 8 µM DOX for 6 h in the presence or absence of APAP (50 µM). A dose-dependent increase in oxidative stress was visualized in all cells after 1 h of treatment. However, a noticeable decrease in fluorescence was seen in cells treated with DOX + APAP (Figure 13). Quantification of mean DCF fluorescence intensity in control and treated cells was also performed. The results confirmed a significant increase in DCF oxidation at all concentrations of DOX after 6 h, relative to baseline measures (Figure 14). At 2 µM and 4 µM concentrations of DOX, cells treated with DOX + APAP showed a significant decrease in oxidant damage as compared to DOX alone. The same trend is seen at 6 µM and 8 µM DOX, although not statistically significant.

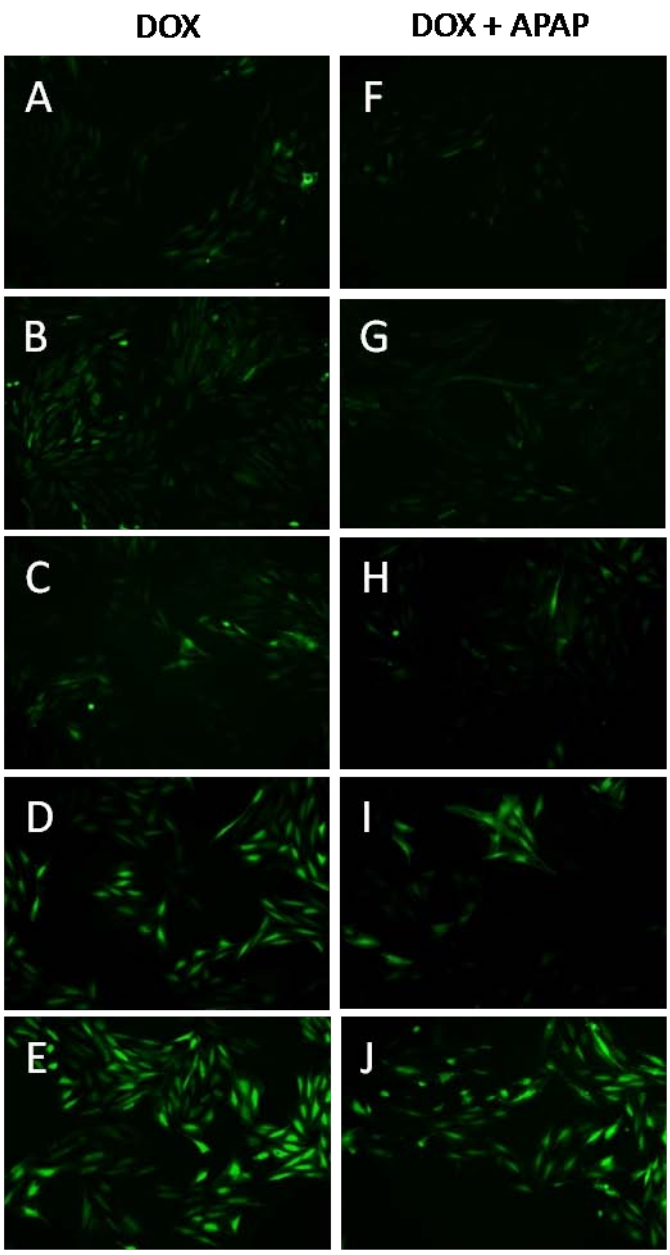

Figure 13: DCF fluorescent images of H9c2 cells upon exposure to DOX. Cells were exposed to different concentrations of DOX (A-J) + 50 µM APAP (F-J): (A,F) 0 µM, (B,G) 2 µM, (C,H) 4 µM, (D,I) 6 µM, (E,J) 8 µM for 2 h, then loaded with DCFH-DA and viewed under fluorescence microscope. APAP-treated cells showed less fluorescence than DOX-only treated cells.

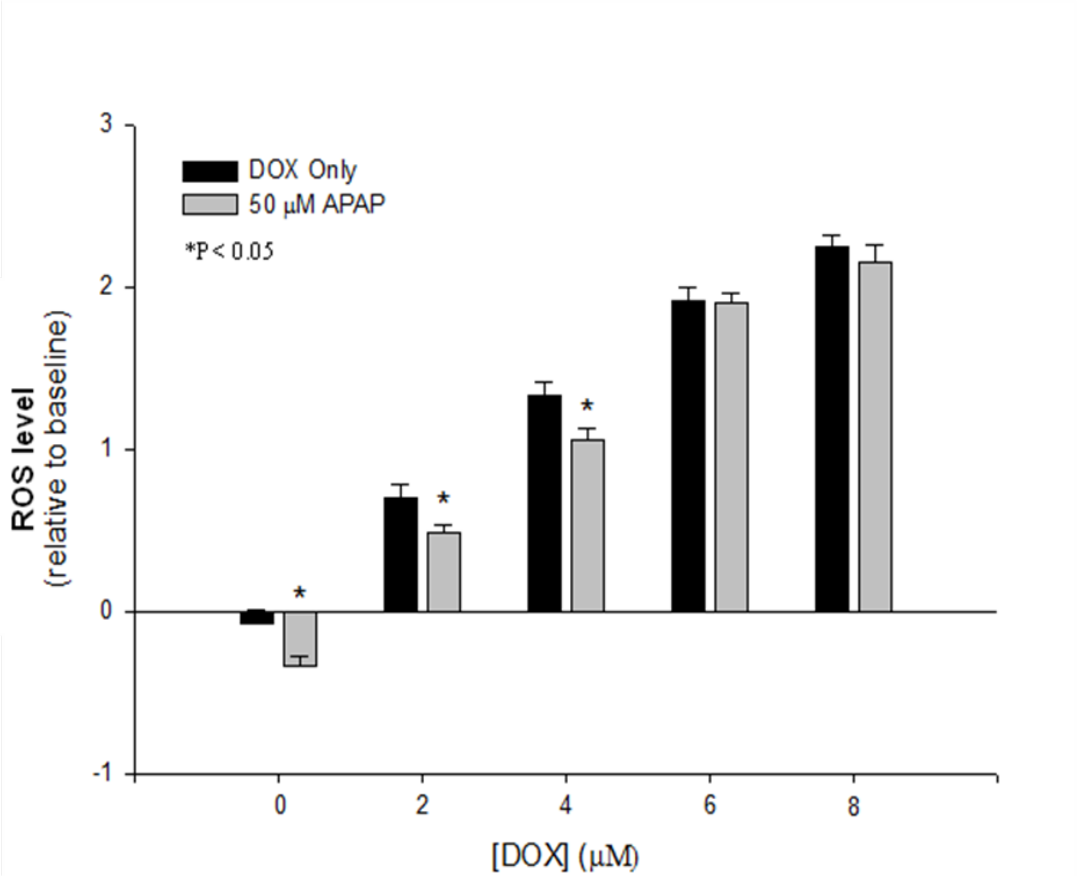

Figure 14: Effect of APAP on ROS levels in DOX treated H9c2 cells. Cells grown to 80% confluence were incubated with DCFH-DA (5 μM), washed with HBSS, and then treated with DOX ± APAP. Measurements of ROS-induced fluorescence were taken every hour for 6 h. DOX significantly increased intracellular ROS production and APAP significantly reduced this effect in cells treated with lower [DOX]. Results represent means of three independent experiments ± SEM. *P < 0.05

2.3 OPN Transcription Levels

To determine whether regulation of OPN synthesis is influenced by DOX, transcript levels were measured in H9c2 cells by RT-PCR. A trend in DOX- dependent increase in OPN transcript level was seen after treatment with 2 µM, 4 µM, 6 µM, and 8 µM DOX. Cells treated with DOX + APAP showed significantly lower levels of OPN than those treated with DOX alone (Figure 15a-b). OPN transcription showed baseline levels at 0.576 in control cells which increased maximally to 0.684 at 4 µM DOX, and decreased to 0.540 in the presence of APAP.

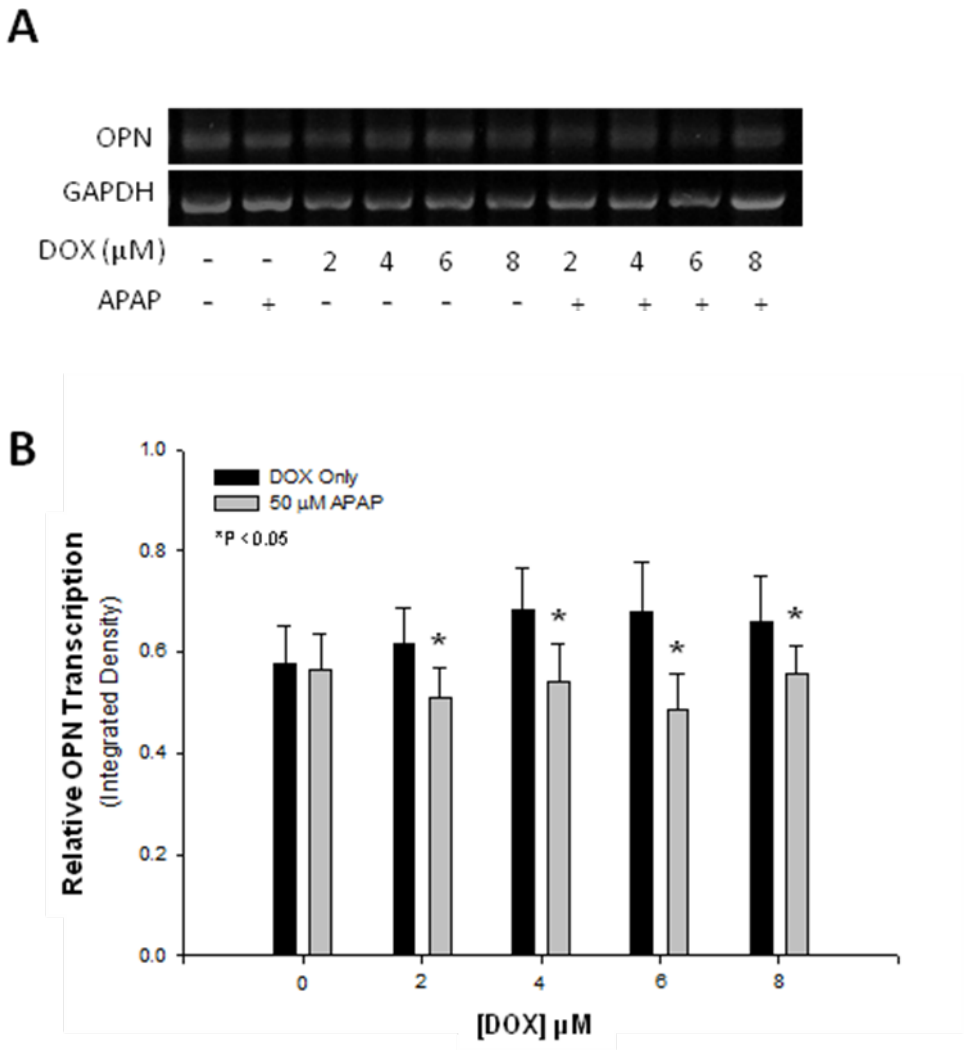

Figure 15: (A) Effect of APAP on OPN transcription after treatment with increasing concentrations of DOX evaluated by RT-PCR using rat gene-specific primers for OPN. Cells grown to 80% confluence were subject to DOX ± APAP for 6 h, media was changed, and cells were allowed to incubate for an additional 18 h in fresh media. (B) Histogram shows DOX increased OPN transcription, which was significantly attenuated by APAP at all concentrations of DOX. Results represent means of 4 independent experiments ± SEM. *P < 0.05

2.4 Dox-Induced Fibrosis

We assessed myocardial fibrosis using Sirius red-stained sections, and found no significant difference in collagen content between control hearts of WT or OPN -/- mice. Nor was there a difference between control and APAP (30 mg/kg) only treated WT or OPN-/- mice. After the cumulative dose of 16 mg/kg DOX over 5 weeks, we found a 4-fold increase in fibrosis in WT mice, and a 3-fold increase in OPN -/- mice compared to control groups. However, groups treated with APAP + DOX had significantly less collagen content than groups treated with DOX alone (WT, 0.029 ± 0.001 vs 0.089 ± 0.003; OPN -/-, 0.036 ± 0.003 vs 0.0779 ± 0.003). Additionally, fibrosis was significantly higher in the DOX group of WT mice as opposed to OPN -/- mice (0.089 ± 0.003 vs. 0.0779 ± 0.003). Figure 16 illustrates the collagen content in the LV free wall of the heart as indicated by the picrosirius red stained tissue portions, and figure 17 is a quantification of the collagen content.

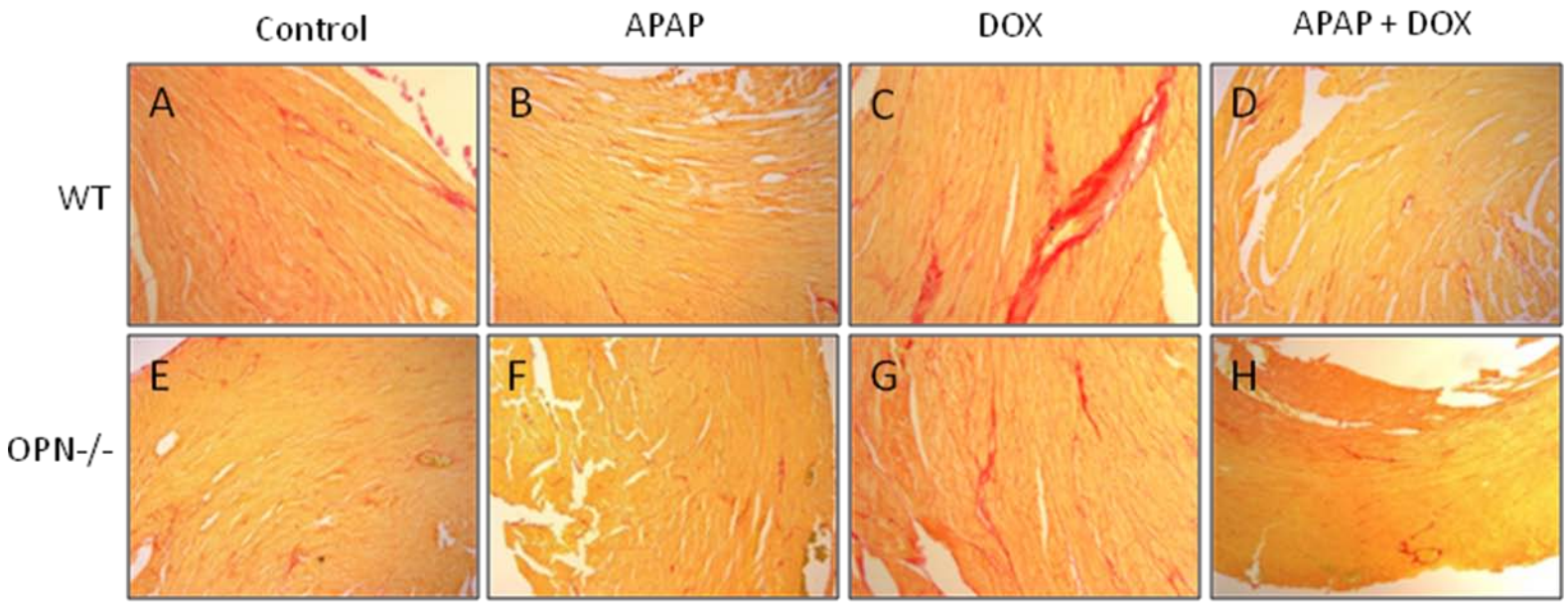

Figure 16: Fibrosis is evident in paraffin tissue sections by increased Sirius red (red stain) within the LV free wall tissue of DOX-treated mice. OPN-/- mice have significantly more left ventricular fibrosis after DOX tretment. Fibrosis in WT and OPN/- mice is significantly attenuated by APAP. Sirius red staining: (A) WT control, (B) WT APAP, (C) WT Dox, (D) WT Dox + APAP, (E) OPN-/- control, (F) OPN-/- APAP, (G) OPN-/- Dox, (H) OPN-/- Dox + APAP.

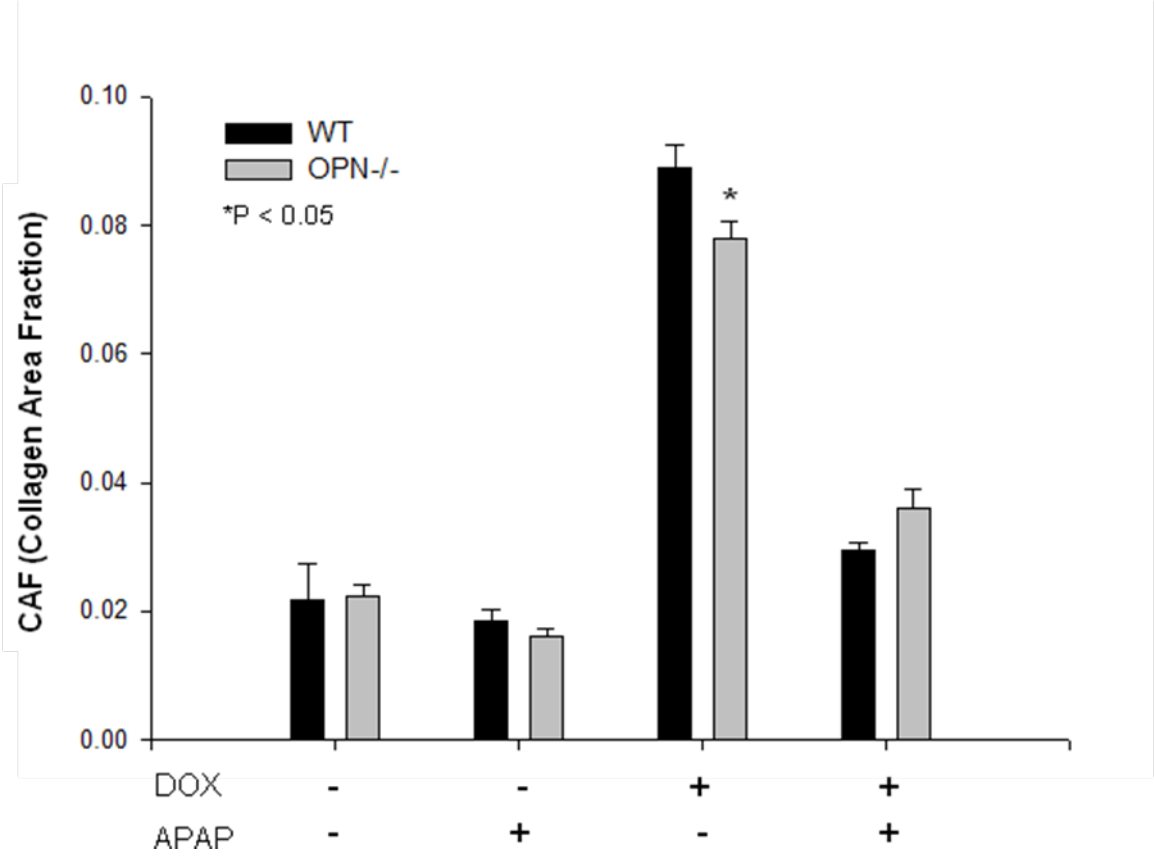

Figure 17: 10-12 wk old male 129 WT and OPN-/- mice subject to IP injection of saline (control) or APAP (30mg/kg) +/- DOX (16 mg/kg). DOX significantly increased the collagen area fraction in both WT and OPN-/- mice, and APAP significantly attenuated that effect. WT mice were significantly more susceptible to DOX-induced fibrosis than OPN-/- mice. *P<0.05 relative to corresponding value for WT.

DISCUSSION

1. ACETAMINOPHEN IN THE H_2O_2-INJURED MYOCARDIUM

1.1 Experimental Protocols

Experiments were conducted to find concentrations of H_2O_2 that would elicit inotropic effects but that would not arrest the heart (data not shown). In most cases we observed a negligible, negative inotropic effect with a concentration of 0.88 mM or smaller, variable inotropic responses at 2.2 mM, and significant changes at concentrations of 6.6 mM, 8.8 mM, and 13.2 mM. Thus we settled on a low (0.88 mM), mid (2.2 mM), and high (6.6 mM) dose to account for inter-dog sensitivity and variability.

1.2 Hemodynamic and Mechanical Properties

A mild dose-dependent biphasic effect was observed in contractile force following treatment with H_2O_2 (data not shown). At μM concentrations there was an initial positive inotropic effect, followed by negative inotropy at mM concentrations. However, after treatment with all concentrations of H_2O_2, acetaminophen-treated dogs showed greater preservation of baseline function when compared to vehicle. Systolic function increased within ten minutes of acetaminophen administration, and remained elevated above baseline levels during H_2O_2 treatment. This unanticipated increase in contractility following treatment with acetaminophen is indicative of positive inotropic compounds, in particular, cardiac glycosides which inhibit the Na^+/K^+ pump and ultimately increase myocyte contractility [111].

Diastolic function did not significantly decrease in APAP-treated dogs following treatment with H_2O_2. However, in H_2O_2-only treated dogs diastolic function significantly declined to 68% of baseline following 6.6 mM H_2O_2. This decreased function is indicative of diminished sarcomere relaxation, a common effect of Ca^{2+} overload, which is absent in APAP-treated dogs. Similar APAP-mediated diastolic preservation was recently observed during hypoxia/reoxygenation in a Langendorf preparation of guinea pig hearts [24]. However, since we did not consider peripheral vascular resistance in these sets of experiments, we cannot rule out the possible effects of acetaminophen on cardiac output, resistance or any other variables relating directly or indirectly to them. To our knowledge, there are no reports of vasoconstriction or hypertension linked to APAP consumption, which would reflect the change in $-dP/dt_{max}$.

Attenuation of H_2O_2-induced lipid peroxidation of myocyte membrane ion channels by APAP could be partially responsible for the results of the current study. Oxidation-induced lipid peroxidation of myocytes is responsible for a wide variety of pathology following myocardial infarction. Lipid peroxidation by ROS often results in damage to Na^+/K^+ pumps [112, 113], Na^+-H^+ exchangers [114-116], and Na^+ [117] and Ca^+ [118] channels, as well as other membrane bound proteins [117]. Recently, Davidenko [119] reported that the reaction of peroxidase in the presence of a phenol leads to polymerization of the phenol, increasing antioxidant capacity, and inactivation of the oxidant. This and other antioxidant studies [19] corroborate our evidence that because APAP is a mono-phenol, it can scavenge ROS and protect channels in part by preventing lipid peroxidation.

1.3 Electrocardiogram

Overall, a significant antiarrhythmic effect was observed in APAP + H_2O_2-treated dogs versus H_2O_2-only-treated dogs. Using exogenous ouabain to induce arrhythmia in dogs, we recently reported similar antiarrhythmic activity of acetaminophen [120], suggesting that acetaminophen's mechanism of protection may involve the Na^+/K^+ pump. Another group has reported a decrease in Na^+/K^+ pump activity following H_2O_2, which is effectively abolished following treatment with other antioxidants [121]. Since the mammalian myocardium contains peroxidase and catalase which catalyze H_2O_2 to produce strong oxidants when in the presence of metals, it is not surprising that H_2O_2 causes cardiac damage and that the antioxidant phenolic properties of acetaminophen minimize the damage to both myocytes and mitochondria. Based on these studies, we hypothesize that acetaminophen attenuates arrhythmias, at least in part, by protecting ion channels and transporters, e.g. the Na^+/K^+ pump, from oxidant damage. More work is needed to clarify the specific target(s) of acetaminophen and its contribution to anti-arrhythmogenesis.

1.4 Plasma concentration of acetaminophen

We chose a dose of 15 mg/kg acetaminophen as a therapeutic concentration in the dog based on the maximum recommended daily dose of Extra Strength Tylenol for humans, 60 mg/kg [5, 19], and on previous clinical studies [1]. Previous studies completed in this laboratory have routinely utilized a divided dose, 15 mg/kg before ischemia and another 15 mg/kg mid-way through reperfusion for a total of 30 mg/kg [22]. The suggested human therapeutic range is 650-1000 mg orally or 10-100 μg/ml in plasma

depending on the study design, route of administration, etc. [5, 122, 123]. Thus, our concentration is in the lower therapeutic range, and is almost completely metabolized in the dog after 3 hours with a peak concentration of 19.1±2 μg/ml at 30 min post administration.

1.5 Myofibrillar ultrastructure

Scanning electron micrographs (SEM) of the epi- and midmyocardium showed a trend in tissue myofibrillar ultrastructure and mitochondrial preservation in H_2O_2 + APAP-treated dogs when compared to H_2O_2-alone. H_2O_2-only-treated hearts showed dilated sarcotubules and numerous vacuoles, which were absent in H_2O_2 + APAP-treated dogs. Contraction bands and liposomes were ubiquitous in H_2O_2-treated hearts, and nearly absent in APAP-treated dogs. The light I-bands and dark Z-lines within the sarcomere were disjointed and blurred in H_2O_2-treated hearts but well-defined in H_2O_2 + APAP-treated hearts. Mitochondria were swollen, rounded, diffusely packed, and contained AMDs in the presence of H_2O_2. With APAP treatment, mitochondria were elongated, non-swollen, dark, lacked AMDs, and were more densely packed. These defining features of damage are indicative of compromised myocyte membrane structure, function and increased mitochondrial permeability, consistent with a higher degree of cellular damage in H_2O_2-treated hearts versus H_2O_2 + APAP-treated [21, 124, 125].

1.6 Concentration of H_2O_2

Previous studies in smaller mammals and cell culture have utilized H_2O_2 concentrations equivalent to the ones we chose. Common concentrations range from

100μM to 1mM [32, 99, 126, 127] depending on the experimental model. The effects of H_2O_2 have also been tested in the diseased human heart. Loh and colleagues [128] tested H_2O_2 on the heart and found a negligible change in cardiac function using 1 mM H_2O_2 and a pronounced effect with a 3 mM solution. For this reason, we chose a range of concentrations to elicit variable effects in the intact canine heart.

Direct measurement of H_2O_2 or OH^- in the blood was not performed in these experiments; we estimated the concentration of circulating H_2O_2 in the blood based on the animals' weight. We estimated that after introducing 0.88 mM of H_2O_2 the concentration of H_2O_2 in the dog was 0.5 mM, after 2.2 mM it was 1.2 mM, and after 6.6 mM the circulating concentration was 3.78 mM. Of course, these estimates do not account for either the kinetics or volume of distribution of H_2O_2 in body water compartments.

1.7 Conclusions

In the canine myocardium exposed to H_2O_2, acetaminophen is cardioprotective. This is evident in the preservation of contractile function, in the maintenance of myofibrillar integrity, and in the attenuation of life-threatening arrhythmias. The preservation by acetaminophen may be mediated by the antioxidant nature of the drug, as previous studies have shown that coronary effluent from APAP-treated hearts subject to ischemia/reperfusion contain less ROS.

2. ACETAMINOPHEN IN THE DOXORUBICIN-INJURED MYOCARDIUM

1.1 Experimental Protocols

Experiments were conducted to find concentrations of DOX that would elicit oxidative stress in the cells and would approximate levels of DOX seen transiently in plasma following pharmaceutical use in patients [54]. The dose of 30 mg/kg APAP chosen for the mice in this study was based on the indicated therapeutic range for APAP in humans as 10-100 μg/ml plasma, which corresponds to a dose of about 1 g every 4 hours for approximately 4 doses in a 50-70 kg patient [129]; although acute pain and fever can be managed with doses of 325-500 mg four times daily. The concentration of 50 μM used for H9c2 experiments was chosen based on previous literature utilizing a 10-500 μM range, and through pilot experiments investigating 10- 200 μM APAP.

1.2 H9c2(2-1): Rat Heart-Derived Embryonic Myoblasts

The rat heart-derived embryonic myoblast cell line was first established and characterized by Kimes and Brandt in 1976 [130]. H9c2(2-1) is a subclone of the original clonal cell line (H9) derived from embryonic BD1X rat heart tissue. It was established using a slight modification of the method of "selective serial passage" described by Yaffe [131, 132].

The primary culture that gave rise to the cell line H9 was obtained from predominantly ventricular tissue of a 13 day embryonic rat heart. From this, a clone was selected which presented spindle-shaped cells that grew in orderly parallel arrays on the surface of tissue culture dishes. The H9c2(2-1) subclone was further selected for

formation of multinucleated tube-like structures. This subclone propagated as a mononucleated myoblast and began to form multinucleated tubular structures upon reaching confluency. The creatine kinase (CK) isoenzymes expressed by this cell line are indicative of skeletal and cardiac muscle types. Both M (muscle) and B (brain) isoenzymes are expressed, with dimer formation patterns indicative of cardiac muscle.

The H9c2 cell line has since become an accepted *in vitro* cellular model for both skeletal and cardiac muscle. Investigation of cardiac hypertrophy, hypoxia, signal transduction, and apoptosis, secondary to oxidant injury (tert-butylhydroperoxide, H_2O_2, doxorubicin, etc) has been extensively studied using H9c2 [133-138]. Studies using primary cultures of rat or mouse ventricular myocytes exposed to oxidants show a similar pattern of cellular response to H_2O_2 as H9c2 cells.

2.3 Reactive Oxygen Species

The specific ROS generated by DOX are somewhat controversial, but most reports agree that the major species are $\cdot O_2^-$ and $OH\cdot$. In the present study, we used DOX to induce intracellular oxidant injury which we measured using FITC fluorescence. Our observations of decreased oxidant stress in the presence of APAP are confirmed in the literature using other models of ROS-inducing injury. For example, Van Dyke *et al.* [139] found that acetaminophen is a potent inhibitor of peroxynitrite-mediated chemiluminescence, and Merrill *et al.* [99] found that coronary effluent samples from acetaminophen-treated hearts exposed to ischemia and reperfusion inhibit peroxynitrite production. Using hypoxic/reoxygenated guinea pig heart, Rork *et al.* [20] demonstrated significantly decreased peroxynitrite-mediated chemiluminescense in coronary effluent

samples, and decreased superoxide-mediated lucigenin chemiluminescense. Therefore, this report confirms earlier reports that acetaminophen exhibits antioxidant capacity and the first, to our knowledge, that directly demonstrates decreased intracellular oxidation.

2.4 Cell Viability & Oxidative Stress in Doxorubicin-Treated Cells

Doxorubicin's intended anti-neoplastic effects target rapidly dividing tumor cells, specifically by inhibition of DNA and RNA synthesis via intercalation in the DNA helix, and topoisomerase inhibition. These anticipated causes of cell death are not directly experienced by the heart, as myocytes are largely non-regenerative. *In vivo*, the major injury sustained by the heart due to DOX exposure is via generation of ROS. In the current studies, however, we chose the H9c2 cell line which is a cardiac myoblast line which proliferates rapidly, unlike its differentiated *in vivo* counterparts. For this reason, when we chose to explore the effect of APAP on DOX-induced cell death as demonstrated by the MTT assay, it was necessary to supplement our data by the DCFH-DA intracellular oxidative stress assay. Our results show that APAP did significantly attenuate DOX-induced cell death at [DOX] of 4 μM, 6 μM, and 8 μM. This trend is similarly observed in the decreased oxidative stress experienced by cells treated with APAP as opposed to DOX alone. We can therefore conclude that the increased viability of APAP-treated cells is, at least in part, attributed to the decreased amount of oxidative stress experienced by the cells.

Interestingly, we see significant preservation in cell viability at high [DOX], yet no significant reduction in oxidative stress at these concentrations. We hypothesize that this may be occurring due to a combination of theories: (1) the antioxidant activity of

APAP is overwhelmed at high [DOX] and thus the preserved viability seen at these higher concentrations is due to other factors such as direct affects on DNA stability, or (2) the viable cell number in DOX-only-treated cells is significantly decreased when compared to DOX + APAP, so the total number of cells contributing to the measured fluorescence is significantly reduced in DOX-only-treated cells, which would account for the overall decreased fluorescence in DOX-only-treated cells as compared to the DOX + APAP treated cells, which have a significantly increased viability and therefore more viable cells to experience any degree of oxidative stress and to add to the fluorescence.

2.5 Ventricular Remodeling: ROS and Fibrosis

The pro-fibrotic effects of ROS are well recognized, involving a multitude of processes including increase in fibroblast proliferation, their transformation into matrix-generating myofibroblasts, the expression of pro-fibrotic genes and alterations in the balance between the activities of matrix destruction (MMPs) and collagen deposition.

A variety of disease states resulting in cardiac fibrosis produce ROS via NADPH oxidase. ROS in the development of cardiac fibrosis *in vivo* has recently been addressed in studies with Nox2 -/- mice. Nox2 is a subunit in the NADPH oxidase enzyme complex. Interstitial cardiac fibrosis occurring in response to a 2-week infusion of angiotensin II was found to be almost completely abolished in these animals [140, 141]. The basis of this effect was an inhibition of increases in the mRNA expression of procollagen I, III and connective tissue growth factor (CTGF), the activation of NF-κB and the activation of MMP-2 in Nox2 -/- mice [141]. In a model of aldosterone-induced interstitial fibrosis, similar results were also obtained using Nox2 -/- mice [141].

Accordingly, Sun *et al.* [142] previously reported that aldosterone-induced interstitial cardiac fibrosis in rats was associated with increased oxidative stress and ventricular Nox2 expression. In the same model as Sun and colleagues, Park *et al.* [143] reported that *in vivo* cardiac fibrosis was inhibited by chronic treatment with an NADPH oxidase inhibitor, apocynin.

In the current study, we used DOX, a chemotherapeutic well known to produce ROS and induce cardiac fibrosis. Our results are consistent with the literature in that the presence of DOX significantly increased the abundance of interstitial collagen. However, this is the first such report that illustrates the anti-fibrotic effects of APAP in the cardiovascular system. The mechanism of action remains to be further investigated, but we hypothesize that its anti-oxidant properties mediate the protection since our results align with those using gene or drug therapeutics which minimize or eradicate oxidant burden.

2.6 Ventricular Remodeling: OPN and Fibrosis

Only low levels of OPN are expressed in healthy cardiac muscle tissue. However, during several pathological states, OPN expression in the heart increases markedly. Increased expression of OPN is shown to be associated with the development of heart failure, and in primary pathological states such as pressure/volume overload, acute MI, LV hypertrophy, and other cadiomyopathy. A variety of cells in the heart are known to express OPN. Although cardiac myocytes occupy 75% of normal heart tissue volume, they only account for 30-40% of the total cell number. The remainder of cells are fibroblasts, endothelial cells and vascular smooth muscle cells.

In one study using WT and OPN-/- mice in an induced MI model, the expression of OPN in infarct regions was primarily localized to nonmuscle and infiltrating cells. Diffuse OPN message was also detectible in the non-infarct LV, with more focal message associated with blood vessels, possibly in endothelial and/or smooth muscle cells [92]. In spontaneously hypertensive rats with heart failure, in situ hybridization of heart sections revealed abundant expression of OPN mRNA, primarily in non-myocytes in the interstitial and perivascular space [144]. In hamsters with heritable cardiomyopathy, increased OPN expression was observed mainly by infiltrating macrophages and was localized to the interstitium [145]. In LV hypertrophy OPN expression is mainly observed in cardiac myocytes [94]. Immunohistochemical analysis of myocardial biopsies obtained from patients with heart failure due to dilated cardiomyopathy (DCM) demonstrated increased OPN expression in cardiac myocytes, which correlated positively with impaired LV function [146], and collagen type I levels [93]. More recently, Yu *et al.* [147] demonstrated parallel increases in IL-18, OPN expression, and interstitial fibrosis in murine models of left ventricular pressure and volume overload.

A well organized extracellular matrix (ECM) plays an important role in maintaining the strength and organization of the cardiac tissue. Mice lacking OPN grow normally but deposit collagen in an abnormal manner with faulty wound healing [148]. Using scanning electron microscopy, Trueblood and colleagues [92] analyzed collagen weave (fibrosis) of WT and OPN -/- mice with induced MI, and similarly found disrupted collagen patterns in the myocardium of sham OPN -/- mice. In post-MI WT mice, large collagen fibers and thin collagen weave was increased in non-infarct LV regions. However, post-MI OPN -/- mice revealed a reduction in both of these types of collagen,

and Northern analysis demonstrated no significant increase in collagen I (α1) mRNA expression. These data, combined with similar results using other models of myocardial remodeling (i.e. aldosterone infusion, streptozotocin diabetic cardiomiopathy, Ang II infusion) suggest that increased OPN expression in the heart post-injury plays a crucial role in regulating LV remodeling, at least in part, by promoting collagen synthesis and accumulation.

Our results indicate that in response to ROS, OPN contributes to cardiac interstitial collagen accumulation *in vivo*. This response is well documented in the literature, however, *in vitro* we report for the first time a trend that APAP negatively regulates RNA levels of OPN in response to DOX, although not significantly. Together these results suggest that APAP indirectly inhibits increased collagen synthesis through negative regulation of OPN transcription.

2.7 Conclusions

Baseline levels of OPN were similar in control and APAP-treated H9c2 cells, and the administration of DOX resulted in a trend of increased transcription, which was attenuated by APAP. The trend of increased OPN transcription correlated positively with DOX-induced oxidative stress, and DOX- induced cell death, both of which were attenuated by APAP. In mice, this similar trend was observed. WT mice exhibited increased DOX-induced fibrosis when compared to OPN-/-. We also found that treatment with APAP attenuated DOX-induced fibrosis in both WT and OPN -/- mice, suggesting that OPN is a non-essential agonist of collagen synthesis and fibrosis. We conclude that acetaminophen exerts its cardioprotective actions, at least in part, by

inhibiting the ROS-mediated activation of OPN and subsequent accumulation of interstitial collagen.

Figure 18 illustrates the past and present recognized effects of APAP on the heart. Together this data suggest that APAP exerts its effect on many proteins, biochemical and cellular processes that are downstream of ROS producing injury. In previous studies by Rork *et al.* [24] and Merrill *et al.* [99], a reduction in peroxynitrite- mediated luminescence was observed in APAP-treated guinea pigs and dogs, respectively. This study corroborates those findings, further strengthening that APAP functions as an intracellular antioxidant, which inhibits any negative downstream alterations in cellular function resulting from injury. Furthermore, this study demonstrates that the cardioprotective effects of APAP are seen immediately after ROS-inducing injury as evidenced by attenuation of H_2O_2 -induced dysfunction, in addition to attenuation of chronic injury such as ventricular fibrosis.

2.8 Future Directions

Further confirmation of altered gene regulation and expression resulting from oxidant injury in the heart would strengthen our current findings. For example, the effects of APAP on GATA4 regulation and subsequent regulation of cardiac sarcomere proteins, and induction of the 'fetal gene program' which occurs parallel to cardiac injury leading to hypertrophy, would be useful to investigate. Investigation of gene expression *in vivo* is the next step in these current studies. Ultimately, we would like to use immunohistochemistry to observe OPN expression and distribution, and GATA4

activation in the hearts of WT mice exposed to DOX ± APAP, and to investigate altered gene expression either by PCR or microarray experiments.

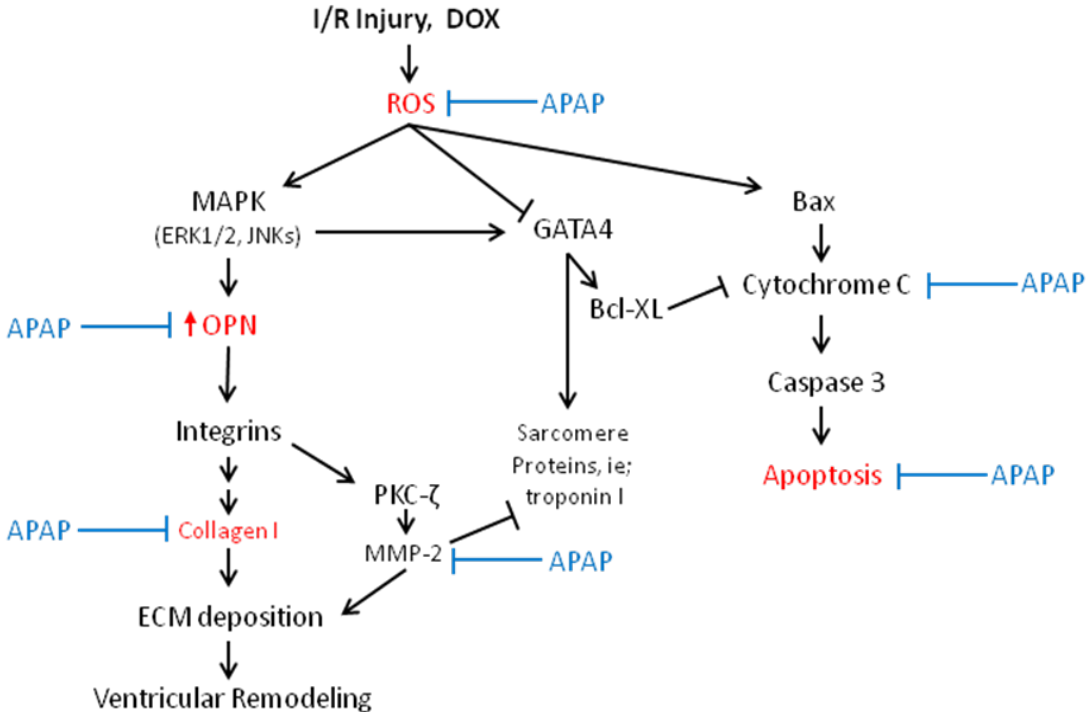

Figure 18: Research summary of the effect of APAP on the heart during oxidant injury. Rork e*t al.* showed inhibition of MMP-2 mediated cleavage of troponin I, Hadzimichalis *et al.* demonstrated protection of the mitochondrial permeability transition pore which attenuated cytochrome *c* induced apoptosis, and the current study confirms decreased ROS-induced OPN-mediated cardiac fibrosis.

REFERENCES

[1] Autret E, Reboul-Marty J, Henry-Launois B, Laborde C, Courcier S, Goehrs JM, *et al.* Evaluation of ibuprofen versus aspirin and paracetamol on efficacy and comfort in children with fever. European journal of clinical pharmacology 1997;51:367-371.

[2] Chandrasekharan NV, Dai H, Roos KL, Evanson NK, Tomsik J, Elton TS, *et al.* COX-3, a cyclooxygenase-1 variant inhibited by acetaminophen and other analgesic/antipyretic drugs: cloning, structure, and expression. Proceedings of the National Academy of Sciences of the United States of America 2002;99:13926-13931.

[3] Pelissier T, Alloui A, Paeile C, Eschalier A. Evidence of a central antinociceptive effect of paracetamol involving spinal 5HT3 receptors. Neuroreport 1995;6:1546-1548.

[4] Merrill G. Acetaminophen (paracetamol) and injury in the cardiovascular system. Vasc Dis Prev 2004; 1.

[5] Prescott LF. Paracetamol (acetaminophen): A critical Bibliographic Review. London: Taylor & Francis, 2001.

[6] Ameer B, Greenblatt DJ. Acetaminophen. Ann Intern Med 1977;87:202-209.

[7] Prescott LF. Paracetamol (Acetaminophen): A Critical Bibliographic Review. New York: Taylor & Francis, 2001.

[8] Baliga SS, Jaques-Robinson KM, Hadzimichalis NM, Golfetti R, Merrill GF. Acetaminophen reduces mitochondrial dysfunction during early cerebral postischemic reperfusion in rats. Brain Res;1319:142-154.

[9] Rahme E, Marentette MA, Kong SX, Lelorier J. Use of NSAIDs, COX-2 inhibitors, and acetaminophen and associated coprescriptions of gastroprotective agents in an elderly population. Arthritis Rheum 2002;47:595-602.

[10] Nakamoto K, Kamisaki Y, Wada K, Kawasaki H, Itoh T. Protective effect of acetaminophen against acute gastric mucosal lesions induced by ischemia-reperfusion in the rat. Pharmacology 1997;54:203-210.

[11] Farquhar WB, Morgan AL, Zambraski EJ, Kenney WL. Effects of acetaminophen and ibuprofen on renal function in the stressed kidney. J Appl Physiol 1999;86:598-604.

[12] Hinson JA, Reid AB, McCullough SS, James LP. Acetaminophen-induced hepatotoxicity: role of metabolic activation, reactive oxygen/nitrogen species, and mitochondrial permeability transition. Drug Metab Rev 2004;36:805-822.

[13] Lores Arnaiz S, Llesuy S, Cutrin JC, Boveris A. Oxidative stress by acute acetaminophen administration in mouse liver. Free radical biology & medicine 1995;19:303-310.

[14] Altinoz MA, Korkmaz R. NF-kappaB, macrophage migration inhibitory factor and cyclooxygenase-inhibitions as likely mechanisms behind the acetaminophen- and NSAID-prevention of the ovarian cancer. Neoplasma 2004;51:239-247.

[15] Peterson JM, Trappe TA, Mylona E, White F, Lambert CP, Evans WJ, *et al.* Ibuprofen and acetaminophen: effect on muscle inflammation after eccentric exercise. Med Sci Sports Exerc 2003;35:892-896.

[16] Golfetti R, Rork T, Merrill G. Chronically administered acetaminophen and the ischemia/reperfused myocardium. Exp Biol Med (Maywood) 2003;228:674-682.

[17] Merrill G, McConnell P, Vandyke K, Powell S. Coronary and myocardial effects of acetaminophen: protection during ischemia-reperfusion. Am J Physiol Heart Circ Physiol 2001;280:H2631-2638.

[18] Golfetti R, VanDyke K, Rork T, Spiler N, Merrill G. Acetaminophen in the post-ischemia reperfused myocardium. Exp Biol Med (Maywood) 2002;227:1031-1037.

[19] Merrill GF, Goldberg E. Antioxidant properties of acetaminophen and cardioprotection. Basic research in cardiology 2001;96:423-430.

[20] Rork TH, Van Dyke K, Spiler NM, Merrill GF. Acetaminophen in the hypoxic and reoxygenated guinea pig myocardium. Experimental biology and medicine (Maywood, NJ 2004;229:1154-1161.

[21] Hadzimichalis NM, Baliga SS, Golfetti R, Jaques KM, Firestein BL, Merrill GF. Acetaminophen-mediated cardioprotection via inhibition of the mitochondrial

permeability transition pore-induced apoptotic pathway. American journal of physiology 2007.

[22] Merrill GF, Rork TH, Spiler NM, Golfetti R. Acetaminophen and myocardial infarction in dogs. American journal of physiology 2004;287:H1913-1920.

[23] Zhu YZ, Chong CL, Chuah SC, Huang SH, Nai HS, Tong HT, *et al.* Cardioprotective effects of nitroparacetamol and paracetamol in acute phase of myocardial infarction in experimental rats. American journal of physiology 2006;290:H517-524.

[24] Rork TH, Hadzimichalis NM, Kappil MA, Merrill GF. Acetaminophen attenuates peroxynitrite-activated matrix metalloproteinase-2-mediated troponin I cleavage in the isolated guinea pig myocardium. Journal of molecular and cellular cardiology 2006;40:553-561.

[25] Antunes F, Cadenas E. Estimation of H2O2 gradients across biomembranes. FEBS Lett 2000;475:121-126.

[26] Nishida M, Maruyama Y, Tanaka R, Kontani K, Nagao T, Kurose H. G alpha(i) and G alpha(o) are target proteins of reactive oxygen species. Nature 2000;408:492-495.

[27] Thannickal VJ, Fanburg BL. Reactive oxygen species in cell signaling. Am J Physiol Lung Cell Mol Physiol 2000;279:L1005-1028.

[28] Sawyer DB, Siwik DA, Xiao L, Pimentel DR, Singh K, Colucci WS. Role of oxidative stress in myocardial hypertrophy and failure. Journal of molecular and cellular cardiology 2002;34:379-388.

[29] Griendling KK, FitzGerald GA. Oxidative stress and cardiovascular injury: Part I: basic mechanisms and in vivo monitoring of ROS. Circulation 2003;108:1912-1916.

[30] Barford D. The role of cysteine residues as redox-sensitive regulatory switches. Curr Opin Struct Biol 2004;14:679-686.

[31] Josephson RA, Silverman HS, Lakatta EG, Stern MD, Zweier JL. Study of the mechanisms of hydrogen peroxide and hydroxyl free radical-induced cellular injury and calcium overload in cardiac myocytes. The Journal of biological chemistry 1991;266:2354-2361.

[32] Horackova M, Ponka P, Byczko Z. The antioxidant effects of a novel iron chelator salicylaldehyde isonicotinoyl hydrazone in the prevention of H(2)O(2) injury in adult cardiomyocytes. Cardiovasc Res 2000;47:529-536.

[33] Goldhaber JI. Free radicals enhance Na+/Ca2+ exchange in ventricular myocytes. The American journal of physiology 1996;271:H823-833.

[34] Wei S, Rothstein EC, Fliegel L, Dell'Italia LJ, Lucchesi PA. Differential MAP kinase activation and Na(+)/H(+) exchanger phosphorylation by H(2)O(2) in rat cardiac myocytes. Am J Physiol Cell Physiol 2001;281:C1542-1550.

[35] Sabri A, Byron KL, Samarel AM, Bell J, Lucchesi PA. Hydrogen peroxide activates mitogen-activated protein kinases and Na+-H+ exchange in neonatal rat cardiac myocytes. Circulation research 1998;82:1053-1062.

[36] Suzuki YJ, Cleemann L, Abernethy DR, Morad M. Glutathione is a cofactor for H2O2-mediated stimulation of Ca2+-induced Ca2+ release in cardiac myocytes. Free radical biology & medicine 1998;24:318-325.

[37] Zweier JL TM. The role of oxidants and free radicals in reperfusion injury. Cardio Res 2006;70:181-190.

[38] Bedard K, Krause KH. The NOX family of ROS-generating NADPH oxidases: physiology and pathophysiology. Physiological reviews 2007;87:245-313.

[39] Becker LB. New concepts in reactive oxygen species and cardiovascular reperfusion physiology. Cardiovasc Res 2004;61:461-470.

[40] Hearse DJ, Humphrey SM, Chain EB. Abrupt reoxygenation of the anoxic potassium-arrested perfused rat heart: a study of myocardial enzyme release. Journal of molecular and cellular cardiology 1973;5:395-407.

[41] Lucas SK, Gardner TJ, Flaherty JT, Bulkley BH, Elmer EB, Gott VL. Beneficial effects of mannitol administration during reperfusion after ischemic arrest. Circulation 1980;62:I34-41.

[42] Stewart JR, Blackwell WH, Crute SL, Loughlin V, Greenfield LJ, Hess ML. Inhibition of surgically induced ischemia/reperfusion injury by oxygen free radical scavengers. J Thorac Cardiovasc Surg 1983;86:262-272.

[43] Jolly SR, Kane WJ, Bailie MB, Abrams GD, Lucchesi BR. Canine myocardial reperfusion injury. Its reduction by the combined administration of superoxide dismutase and catalase. Circulation research 1984;54:277-285.

[44] Burton KP, McCord JM, Ghai G. Myocardial alterations due to free-radical generation. The American journal of physiology 1984;246:H776-783.

[45] Ytrehus K, Myklebust R, Mjos OD. Influence of oxygen radicals generated by xanthine oxidase in the isolated perfused rat heart. Cardiovasc Res 1986;20:597-603.

[46] Zweier JL, Flaherty JT, Weisfeldt ML. Direct measurement of free radical generation following reperfusion of ischemic myocardium. Proceedings of the National Academy of Sciences of the United States of America 1987;84:1404-1407.

[47] Flaherty JT, Zweier JL. Does Lethal Myocardial Reperfusion Injury Exist? J Thromb Thrombolysis 1997;4:91-93.

[48] Chen EP, Bittner HB, Davis RD, Folz RJ, Van Trigt P. Extracellular superoxide dismutase transgene overexpression preserves postischemic myocardial function in isolated murine hearts. Circulation 1996;94:II412-417.

[49] Goldhaber JI, Ji S, Lamp ST, Weiss JN. Effects of exogenous free radicals on electromechanical function and metabolism in isolated rabbit and guinea pig ventricle. Implications for ischemia and reperfusion injury. The Journal of clinical investigation 1989;83:1800-1809.

[50] Unverferth DV, Magorien RD, Unverferth BP, Talley RL, Balcerzak SP, Baba N. Human myocardial morphologic and functional changes in the first 24 hours after doxorubicin administration. Cancer Treat Rep 1981;65:1093-1097.

[51] Sawyer DB, Fukazawa R, Arstall MA, Kelly RA. Daunorubicin-induced apoptosis in rat cardiac myocytes is inhibited by dexrazoxane. Circulation research 1999;84:257-265.

[52] Arola OJ, Saraste A, Pulkki K, Kallajoki M, Parvinen M, Voipio-Pulkki LM. Acute doxorubicin cardiotoxicity involves cardiomyocyte apoptosis. Cancer Res 2000;60:1789-1792.

[53] Childs AC, Phaneuf SL, Dirks AJ, Phillips T, Leeuwenburgh C. Doxorubicin treatment in vivo causes cytochrome C release and cardiomyocyte apoptosis, as well as increased mitochondrial efficiency, superoxide dismutase activity, and Bcl-2:Bax ratio. Cancer Res 2002;62:4592-4598.

[54] Green PS, Leeuwenburgh C. Mitochondrial dysfunction is an early indicator of doxorubicin-induced apoptosis. Biochim Biophys Acta 2002;1588:94-101.

[55] Buzdar AU, Marcus C, Smith TL, Blumenschein GR. Early and delayed clinical cardiotoxicity of doxorubicin. Cancer 1985;55:2761-2765.

[56] Pouna P, Bonoron-Adele S, Gouverneur G, Tariosse L, Besse P, Robert J. Development of the model of rat isolated perfused heart for the evaluation of anthracycline cardiotoxicity and its circumvention. Br J Pharmacol 1996;117:1593-1599.

[57] Wolter KG, Hsu YT, Smith CL, Nechushtan A, Xi XG, Youle RJ. Movement of Bax from the cytosol to mitochondria during apoptosis. J Cell Biol 1997;139:1281-1292.

[58] Marcillat O, Zhang Y, Davies KJ. Oxidative and non-oxidative mechanisms in the inactivation of cardiac mitochondrial electron transport chain components by doxorubicin. The Biochemical journal 1989;259:181-189.

[59] Vasquez-Vivar J, Kalyanaraman B, Kennedy MC. Mitochondrial aconitase is a source of hydroxyl radical. An electron spin resonance investigation. The Journal of biological chemistry 2000;275:14064-14069.

[60] Rajagopalan S, Politi PM, Sinha BK, Myers CE. Adriamycin-induced free radical formation in the perfused rat heart: implications for cardiotoxicity. Cancer Res 1988;48:4766-4769.

[61] Lipshultz SE, Rifai N, Sallan SE, Lipsitz SR, Dalton V, Sacks DB, *et al.* Predictive value of cardiac troponin T in pediatric patients at risk for myocardial injury. Circulation 1997;96:2641-2648.

[62] Charron F, Nemer M. GATA transcription factors and cardiac development. Semin Cell Dev Biol 1999;10:85-91.

[63] Charron F, Paradis P, Bronchain O, Nemer G, Nemer M. Cooperative interaction between GATA-4 and GATA-6 regulates myocardial gene expression. Mol Cell Biol 1999;19:4355-4365.

[64] Grillot DA, Gonzalez-Garcia M, Ekhterae D, Duan L, Inohara N, Ohta S, *et al.* Genomic organization, promoter region analysis, and chromosome localization of the mouse bcl-x gene. J Immunol 1997;158:4750-4757.

[65] Kobayashi S, Volden P, Timm D, Mao K, Xu X, Liang Q. Transcription factor GATA4 inhibits doxorubicin-induced autophagy and cardiomyocyte death. The Journal of biological chemistry;285:793-804.

[66] Murphy AM, Thompson WR, Peng LF, Jones L, 2nd. Regulation of the rat cardiac troponin I gene by the transcription factor GATA-4. The Biochemical journal 1997;322 (Pt 2):393-401.

[67] Chen Y, Jungsuwadee P, Vore M, Butterfield DA, St Clair DK. Collateral damage in cancer chemotherapy: oxidative stress in nontargeted tissues. Mol Interv 2007;7:147-156.

[68] Kim Y, Ma AG, Kitta K, Fitch SN, Ikeda T, Ihara Y, *et al.* Anthracycline-induced suppression of GATA-4 transcription factor: implication in the regulation of cardiac myocyte apoptosis. Mol Pharmacol 2003;63:368-377.

[69] Kwon SH, Pimentel DR, Remondino A, Sawyer DB, Colucci WS. H(2)O(2) regulates cardiac myocyte phenotype via concentration-dependent activation of distinct kinase pathways. Journal of molecular and cellular cardiology 2003;35:615-621.

[70] Yamaguchi O, Higuchi Y, Hirotani S, Kashiwase K, Nakayama H, Hikoso S, *et al.* Targeted deletion of apoptosis signal-regulating kinase 1 attenuates left ventricular remodeling. Proceedings of the National Academy of Sciences of the United States of America 2003;100:15883-15888.

[71] Boraso A, Williams AJ. Modification of the gating of the cardiac sarcoplasmic reticulum Ca(2+)-release channel by H2O2 and dithiothreitol. The American journal of physiology 1994;267:H1010-1016.

[72] Suzuki YJ, Monterubio, J., Hughes, B.A., Cleemann, L., Abernethy, D. R., Morad M. Hydrogen peroxide regulates the ryanodine receptor and the Na+-Ca2+ exchanger in rat (Rattus norvegicus) cardiac myocytes. Bulletin MDIBL 1996;35:33-34.

[73] Wang SY, Clague JR, Langer GA. Increase in calcium leak channel activity by metabolic inhibition or hydrogen peroxide in rat ventricular myocytes and its inhibition by polycation. Journal of molecular and cellular cardiology 1995;27:211-222.

[74] Song Y, Shryock JC, Wagner S, Maier LS, Belardinelli L. Blocking late sodium current reduces hydrogen peroxide-induced arrhythmogenic activity and contractile dysfunction. The Journal of pharmacology and experimental therapeutics 2006;318:214-222.

[75] Swain SM, Whaley FS, Ewer MS. Congestive heart failure in patients treated with doxorubicin: a retrospective analysis of three trials. Cancer 2003;97:2869-2879.

[76] Murdoch CE, Zhang M, Cave AC, Shah AM. NADPH oxidase-dependent redox signalling in cardiac hypertrophy, remodelling and failure. Cardiovasc Res 2006;71:208-215.

[77] Murdoch CE, Grieve DJ, Cave AC, Looi YH, Shah AM. NADPH oxidase and heart failure. Curr Opin Pharmacol 2006;6:148-153.

[78] Engberding N, Spiekermann S, Schaefer A, Heineke A, Wiencke A, Muller M, *et al.* Allopurinol attenuates left ventricular remodeling and dysfunction after experimental myocardial infarction: a new action for an old drug? Circulation 2004;110:2175-2179.

[79] Streeter DD, Jr., Vaishnav RN, Patel DJ, Spotnitz HM, Ross J, Jr., Sonnenblick EH. Stress distribution in the canine left ventricle during diastole and systole. Biophys J 1970;10:345-363.

[80] Streeter DD, Jr., Spotnitz HM, Patel DP, Ross J, Jr., Sonnenblick EH. Fiber orientation in the canine left ventricle during diastole and systole. Circulation research 1969;24:339-347.

[81] Goldsmith EC, Carver W, McFadden A, Goldsmith JG, Price RL, Sussman M, *et al.* Integrin shedding as a mechanism of cellular adaptation during cardiac growth. American journal of physiology 2003;284:H2227-2234.

[82] Burgess ML, Carver WE, Terracio L, Wilson SP, Wilson MA, Borg TK. Integrin-mediated collagen gel contraction by cardiac fibroblasts. Effects of angiotensin II. Circulation research 1994;74:291-298.

[83] Baumgarten G, Knuefermann P, Kalra D, Gao F, Taffet GE, Michael L, *et al.* Load-dependent and -independent regulation of proinflammatory cytokine and cytokine receptor gene expression in the adult mammalian heart. Circulation 2002;105:2192-2197.

[84] Booz GW, Baker KM. Molecular signalling mechanisms controlling growth and function of cardiac fibroblasts. Cardiovasc Res 1995;30:537-543.

[85] Hsueh WA, Law RE, Do YS. Integrins, adhesion, and cardiac remodeling. Hypertension 1998;31:176-180.

[86] Denhardt DT, Noda M, O'Regan AW, Pavlin D, Berman JS. Osteopontin as a means to cope with environmental insults: regulation of inflammation, tissue remodeling, and cell survival. The Journal of clinical investigation 2001;107:1055-1061.

[87] Gladson CL, Stewart JE, Olman MA, Chang PL, Schnapp LM, Grammer JR, *et al.* Attachment of primary neonatal rat astrocytes to vitronectin is mediated by integrins alphavbeta5 and alpha8beta1: modulation by the type 1 plasminogen activator inhibitor. Neurosci Lett 2000;283:157-161.

[88] Liaw L, Skinner MP, Raines EW, Ross R, Cheresh DA, Schwartz SM, *et al.* The adhesive and migratory effects of osteopontin are mediated via distinct cell surface integrins. Role of alpha v beta 3 in smooth muscle cell migration to osteopontin in vitro. The Journal of clinical investigation 1995;95:713-724.

[89] Ross RS, Pham C, Shai SY, Goldhaber JI, Fenczik C, Glembotski CC, *et al.* Beta1 integrins participate in the hypertrophic response of rat ventricular myocytes. Circulation research 1998;82:1160-1172.

[90] Zohar R, Zhu B, Liu P, Sodek J, McCulloch CA. Increased cell death in osteopontin-deficient cardiac fibroblasts occurs by a caspase-3-independent pathway. American journal of physiology 2004;287:H1730-1739.

[91] Kossmehl P, Schonberger J, Shakibaei M, Faramarzi S, Kurth E, Habighorst B, *et al.* Increase of fibronectin and osteopontin in porcine hearts following ischemia and reperfusion. Journal of molecular medicine (Berlin, Germany) 2005;83:626-637.

[92] Trueblood NA, Xie Z, Communal C, Sam F, Ngoy S, Liaw L, *et al.* Exaggerated left ventricular dilation and reduced collagen deposition after myocardial infarction in mice lacking osteopontin. Circulation research 2001;88:1080-1087.

[93] Satoh M, Nakamura M, Akatsu T, Shimoda Y, Segawa I, Hiramori K. Myocardial osteopontin expression is associated with collagen fibrillogenesis in human dilated cardiomyopathy. Eur J Heart Fail 2005;7:755-762.

[94] Graf K, Do YS, Ashizawa N, Meehan WP, Giachelli CM, Marboe CC, *et al.* Myocardial osteopontin expression is associated with left ventricular hypertrophy. Circulation 1997;96:3063-3071.

[95] Matsui Y, Jia N, Okamoto H, Kon S, Onozuka H, Akino M, *et al.* Role of osteopontin in cardiac fibrosis and remodeling in angiotensin II-induced cardiac hypertrophy. Hypertension 2004;43:1195-1201.

[96] Zhao X, Johnson JN, Singh K, Singh M. Impairment of myocardial angiogenic response in the absence of osteopontin. Microcirculation 2007;14:233-240.

[97] Siwik DA, Colucci WS. Regulation of matrix metalloproteinases by cytokines and reactive oxygen/nitrogen species in the myocardium. Heart failure reviews 2004;9:43-51.

[98] Slezak J, Tribulova N, Pristacova J, Uhrik B, Thomas T, Khaper N, *et al.* Hydrogen peroxide changes in ischemic and reperfused heart. Cytochemistry and biochemical and X-ray microanalysis. Am J Pathol 1995;147:772-781.

[99] Merrill GF. Acetaminophen and low-flow myocardial ischemia: efficacy and antioxidant mechanisms. American journal of physiology 2002;282:H1341-1349.

[100] Karmazyn M, Pierce GN, Williams S. Effect of nonsteroidal anti-inflammatory drugs on the hypoxic rat heart. The Journal of pharmacology and experimental therapeutics 1981;218:488-496.

[101] Teng RJ, Ye YZ, Parks DA, Beckman JS. Urate produced during hypoxia protects heart proteins from peroxynitrite-mediated protein nitration. Free radical biology & medicine 2002;33:1243-1249.

[102] Suliman HB, Carraway MS, Ali AS, Reynolds CM, Welty-Wolf KE, Piantadosi CA. The CO/HO system reverses inhibition of mitochondrial biogenesis and prevents murine doxorubicin cardiomyopathy. The Journal of clinical investigation 2007;117:3730-3741.

[103] Simunek T, Sterba M, Popelova O, Adamcova M, Hrdina R, Gersl V. Anthracycline-induced cardiotoxicity: overview of studies examining the roles of oxidative stress and free cellular iron. Pharmacol Rep 2009;61:154-171.

[104] Jalil JE, Doering CW, Janicki JS, Pick R, Shroff SG, Weber KT. Fibrillar collagen and myocardial stiffness in the intact hypertrophied rat left ventricle. Circulation research 1989;64:1041-1050.

[105] Turakhia S, Venkatakrishnan CD, Dunsmore K, Wong H, Kuppusamy P, Zweier JL, *et al.* Doxorubicin-induced cardiotoxicity: direct correlation of cardiac fibroblast and H9c2 cell survival and aconitase activity with heat shock protein 27. American journal of physiology 2007;293:H3111-3121.

[106] Oyama Y, Hayashi A, Ueha T, Maekawa K. Characterization of 2',7'-dichlorofluorescin fluorescence in dissociated mammalian brain neurons: estimation on intracellular content of hydrogen peroxide. Brain research 1994;635:113-117.

[107] Park EJ, Park K. Induction of reactive oxygen species and apoptosis in BEAS-2B cells by mercuric chloride. Toxicol In Vitro 2007;21:789-794.

[108] Jaques-Robinson KM, Golfetti R, Baliga SS, Hadzimichalis NM, Merrill GF. Acetaminophen is cardioprotective against H2O2-induced injury in vivo. Experimental biology and medicine (Maywood, NJ 2008;233:1315-1322.

[109] Lucchesi BR, Hardman HF. The influence of dichloroiso-proterenol (DCI) and related compounds upon ouabain and acetylstrophanthidin induced cardiac arrhythmias. The Journal of pharmacology and experimental therapeutics 1961;132:372-381.

[110] Walker MJ, Curtis MJ, Hearse DJ, Campbell RW, Janse MJ, Yellon DM, *et al.* The Lambeth Conventions: guidelines for the study of arrhythmias in ischaemia infarction, and reperfusion. Cardiovasc Res 1988;22:447-455.

[111] Manunta P, Ferrandi M. Cardiac glycosides and cardiomyopathy. Hypertension 2006;47:343-344.

[112] Shao Q, Matsubara T, Bhatt SK, Dhalla NS. Inhibition of cardiac sarcolemma Na(+)-K+ ATPase by oxyradical generating systems. Molecular and cellular biochemistry 1995;147:139-144.

[113] Tokube K, Kiyosue T, Arita M. Openings of cardiac KATP channel by oxygen free radicals produced by xanthine oxidase reaction. The American journal of physiology 1996;271:H478-489.

[114] Gumina RJ, Terzic A, Gross GJ. Do NHE inhibition and ischemic preconditioning convey cardioprotection through a common mechanism? Basic research in cardiology 2001;96:318-324.

[115] Doggrell SA, Hancox JC. Is timing everything? Therapeutic potential of modulators of cardiac Na(+) transporters. Expert opinion on investigational drugs 2003;12:1123-1142.

[116] Masereel B, Pochet L, Laeckmann D. An overview of inhibitors of Na(+)/H(+) exchanger. European journal of medicinal chemistry 2003;38:547-554.

[117] Fukuda K, Davies SS, Nakajima T, Ong BH, Kupershmidt S, Fessel J, *et al.* Oxidative mediated lipid peroxidation recapitulates proarrhythmic effects on cardiac sodium channels. Circulation research 2005;97:1262-1269.

[118] Gill JS, McKenna WJ, Camm AJ. Free radicals irreversibly decrease Ca2+ currents in isolated guinea-pig ventricular myocytes. European journal of pharmacology 1995;292:337-340.

[119] Davidenko TI. [Peroxidase oxidation of phenols]. Prikladnaia biokhimiia i mikrobiologiia 2004;40:625-629.

[120] Merrill GF, Merrill JH, Golfetti R, Jaques KM, Hadzimichalis NS, Baliga SS, *et al.* Antiarrhythmic properties of acetaminophen in the dog. Experimental biology and medicine (Maywood, NJ 2007;232:1245-1252.

[121] Kourie JI. Interaction of reactive oxygen species with ion transport mechanisms. The American journal of physiology 1998;275:C1-24.

[122] Rumack BH, Peterson RC, Koch GG, Amara IA. Acetaminophen overdose. 662 cases with evaluation of oral acetylcysteine treatment. Archives of internal medicine 1981;141:380-385.

[123] Prescott LF. Paracetamol: past, present, and future. American journal of therapeutics 2000;7:143-147.

[124] Hearse DJ, Humphrey SM, Nayler WG, Slade A, Border D. Ultrastructural damage associated with reoxygenation of the anoxic myocardium. Journal of molecular and cellular cardiology 1975;7:315-324.

[125] Hegstad AC, Ytrehus K, Lindal S, Myklebust R, Jorgensen L. The initial phase of myocardial reperfusion is not associated with aggravation of ischemic-induced ultrastructural alterations in isolated rat hearts exposed to prolonged global ischemia. Ultrastructural pathology 1999;23:93-105.

[126] Bogoyevitch MA, Ng DC, Court NW, Draper KA, Dhillon A, Abas L. Intact mitochondrial electron transport function is essential for signalling by hydrogen peroxide in cardiac myocytes. Journal of molecular and cellular cardiology 2000;32:1469-1480.

[127] Chen QM, Tu VC, Wu Y, Bahl JJ. Hydrogen peroxide dose dependent induction of cell death or hypertrophy in cardiomyocytes. Archives of biochemistry and biophysics 2000;373:242-248.

[128] Loh SH, Tsai CS, Tsai Y, Chen WH, Hong GJ, Wei J, *et al.* Hydrogen peroxide-induced intracellular acidosis and electromechanical inhibition in the diseased human ventricular myocardium. European journal of pharmacology 2002;443:169-177.

[129] Rumack BH. Acetaminophen misconceptions. Hepatology 2004;40:10-15.

[130] Kimes BW, Brandt BL. Properties of a clonal muscle cell line from rat heart. Exp Cell Res 1976;98:367-381.

[131] Richler C, Yaffe D. The in vitro cultivation and differentiation capacities of myogenic cell lines. Dev Biol 1970;23:1-22.

[132] Yaffe D. Retention of differentiation potentialities during prolonged cultivation of myogenic cells. Proceedings of the National Academy of Sciences of the United States of America 1968;61:477-483.

[133] Wang Z, Cui M, Sun L, Jia Z, Bai Y, Ma K, *et al.* Angiopoietin-1 protects H9c2 cells from H2O2-induced apoptosis through AKT signaling. Biochem Biophys Res Commun 2007;359:685-690.

[134] Spallarossa P, Garibaldi S, Altieri P, Fabbi P, Manca V, Nasti S, *et al.* Carvedilol prevents doxorubicin-induced free radical release and apoptosis in cardiomyocytes in vitro. Journal of molecular and cellular cardiology 2004;37:837-846.

[135] Liu CJ, Cheng YC, Lee KW, Hsu HH, Chu CH, Tsai FJ, *et al.* Lipopolysaccharide induces cellular hypertrophy through calcineurin/NFAT-3 signaling pathway in H9c2 myocardiac cells. Molecular and cellular biochemistry 2008;313:167-178.

[136] Stathopoulou K, Beis I, Gaitanaki C. MAPK signaling pathways are needed for survival of H9c2 cardiac myoblasts under extracellular alkalosis. American journal of physiology 2008;295:H1319-H1329.

[137] Ihara Y, Urata Y, Goto S, Kondo T. Role of calreticulin in the sensitivity of myocardiac H9c2 cells to oxidative stress caused by hydrogen peroxide. Am J Physiol Cell Physiol 2006;290:C208-221.

[138] Bingham AJ, Ooi L, Kozera L, White E, Wood IC. The repressor element 1-silencing transcription factor regulates heart-specific gene expression using multiple chromatin-modifying complexes. Mol Cell Biol 2007;27:4082-4092.

[139] Van Dyke K, Sacks M, Qazi N. A new screening method to detect water-soluble antioxidants: acetaminophen (Tylenol) and other phenols react as antioxidants and destroy peroxynitrite-based luminol-dependent chemiluminescence. J Biolumin Chemilumin 1998;13:339-348.

[140] Bendall JK, Cave AC, Heymes C, Gall N, Shah AM. Pivotal role of a gp91(phox)-containing NADPH oxidase in angiotensin II-induced cardiac hypertrophy in mice. Circulation 2002;105:293-296.

[141] Johar S, Cave AC, Narayanapanicker A, Grieve DJ, Shah AM. Aldosterone mediates angiotensin II-induced interstitial cardiac fibrosis via a Nox2-containing NADPH oxidase. FASEB J 2006;20:1546-1548.

[142] Sun Y, Zhang J, Lu L, Chen SS, Quinn MT, Weber KT. Aldosterone-induced inflammation in the rat heart : role of oxidative stress. Am J Pathol 2002;161:1773-1781.

[143] Park YM, Park MY, Suh YL, Park JB. NAD(P)H oxidase inhibitor prevents blood pressure elevation and cardiovascular hypertrophy in aldosterone-infused rats. Biochem Biophys Res Commun 2004;313:812-817.

[144] Singh K, Sirokman G, Communal C, Robinson KG, Conrad CH, Brooks WW, *et al.* Myocardial osteopontin expression coincides with the development of heart failure. Hypertension 1999;33:663-670.

[145] Murry CE, Giachelli CM, Schwartz SM, Vracko R. Macrophages express osteopontin during repair of myocardial necrosis. Am J Pathol 1994;145:1450-1462.

[146] Stawowy P, Blaschke F, Pfautsch P, Goetze S, Lippek F, Wollert-Wulf B, *et al.* Increased myocardial expression of osteopontin in patients with advanced heart failure. Eur J Heart Fail 2002;4:139-146.

[147] Yu Q, Vazquez R, Khojeini EV, Patel C, Venkataramani R, Larson DF. IL-18 induction of osteopontin mediates cardiac fibrosis and diastolic dysfunction in mice. American journal of physiology 2009;297:H76-85.

[148] Liaw L, Birk DE, Ballas CB, Whitsitt JS, Davidson JM, Hogan BL. Altered wound healing in mice lacking a functional osteopontin gene (spp1). The Journal of clinical investigation 1998;101:1468-1478.

Curriculum Vitae

KATHRYN M. JAQUES

EDUCATION

Ph.D., 2010 Physiology and Integrative Biology

B.S., 2005 University of California Davis
College of Agricultural and Environmental Sciences
Davis, California
Neurobiology, Physiology, and Behavior

PUBLICATIONS

2010 Baliga SS, **Jaques-Robinson KM,** Hadzimichalis NM, Golfetti R, Merrill GF. Acetaminophen reduces mitochondrial dysfunction during early cerebral postischemic reperfusion in rats. *Brain Res.* 2010 Jan 14.

2009 Chakir K, Daya SK, Aiba T, Tunin RS, Dimaano VL, Abraham TP, **Jaques-Robinson KM**, Lai EW, Pacak K, Zhu W, Xiao R, Tomaselli GF, Kass DA. Mechanisms of enhanced beta-adrenergic reserve from cardiac resynchronization therapy. *Circulation*. 2009 Mar 10;119(9):1231-40. Epub 2009 Feb 23.

2008 **Jaques-Robinson KM,** Golfetti R, Baliga S, Hadzimichalis NM, Merrill GF. Acetaminophen is cardioprotective against H_2O_2- induced injury *in vivo*. *Exp Biol Med (Maywood).* 2008 Oct;233(10):1315-22.

2007 Hadzimichalis NM, Baliga SS, Golfetti R, **Jaques KM**, Firestein, BL, Merrill GF. Acetaminophen-mediated cardioprotection via inhibition of the mitochondrial permeability transition pore induced apoptotic pathway. *Am J Physiol Heart Circ Physiol*. 2007 Dec;293(6):H3348-55.

2007 Merrill GF, Merrill J, Golfetti R, **Jaques KM**, Spiler-Hadzimichalis NM, Baliga S, Rork T. Antiarrhythmic Properties of Acetaminophen in the Dog. *Exp Biol Med (Maywood).* 2007 Oct; 232:1245-1252